AN INVESTIGATION OF THE EUROPIUM OXIDEFLUORIDE - EUROPIUM SESQUIOXIDE SYSTEM

Thesis for the Degree of M. S.
MICHIGAN STATE UNIVERSITY
SANDRA LEONARD BACON
1971

OXID

In an a

oxidefluorid

europium ses

This solutio

at constant

sesquioxide

not undergo

above the no

The mod

apparent rea

with either

appeared as

Investi

$EuF_3(s)$ reve

vaporization

A new c

produced by

The structur

9.590 ± 0.00

by chemical

AN INVESTIGATION OF THE EUROPIUM OXIDEFLUORIDE - EUROPIUM SESQUIOXIDE SYSTEM

By

Sandra Leonard Bacon

In an attempt to study the vaporization behavior of europium oxidefluoride, it was learned that the equilibrium product, cubic europium sesquioxide, forms a solid solution with the oxidefluoride. This solution was characterized by a continuous decrease in pressure at constant temperature as the conversion of oxidefluoride to sesquioxide took place and also by the fact that the sesquioxide did not undergo its cubic to monoclinic transition at temperature 300° above the normal transition point.

The mode of vaporization for EuOF was not established due to apparent reaction of molybdenum, tungsten, thoria and platinum cells with either the residue or effusate. Condensed effusate always appeared as a reduced fluoride $EuF_{2.3}$.

Investigation into the reactions of molybdenum and platinum with $EuF_3(s)$ revealed that some reduction occurs in the solid state during vaporization at 1500° in both cases.

A new compound with the proposed formula $Eu_3Th_2(EuO_4)_3O$ was produced by reaction of ThO_2 and EuOF under vaporization conditions. The structure of this compound fits the apatite family with $a = 9.590 \pm 0.002$ Å and $c = 7.065 \pm 0.009$ Å. Confirmation of the formula by chemical analysis has not been completed.

AN INVESTIGATION OF THE EUROPIUM OXIDEFLUORIDE - EUROPIUM SESQUIOXIDE SYSTEM

By

Sandra Leonard Bacon

A THESIS

Submitted to
Michigan State University
in partial fulfillment of the requirements
for the degree of

MASTER OF SCIENCE

Department of Chemistry

1971

The aut
Dr. Harry A.
this investi
Temperature
C. Biefeld i

To the
so patient.

The fina
U. S. Atomic

ACKNOWLEDGMENTS

The author wishes to express her sincere appreciation to Dr. Harry A. Eick for his guidance and assistance in the course of this investigation. Also, the aid of the members of the High Temperature Group, Dr. R. Seivers, D. E. Work, A. V. Hariharan and C. Biefeld is most gratefully acknowledged.

To the author's husband, Terrance, a special thanks for being so patient.

The financial support of the National Science Foundation and U. S. Atomic Energy Commission is gratefully acknowledged.

TABLE OF CONTENTS

I. Wei

II. Inte
Effu

III. Repo

TABLE OF TABLES

The e
attributed
oxidefluor
Zachariase
except tho
accepted as
found by K
Both stoich
the cubic p
structure m
temperature
relatively

Other s
of nonstoich
in which $0 \le x$
where $0.5 \le x$
In some case
others[6] an o
distortion m
present in th
of fluoride i
region of sol
trifluoride.[3]

I. Introduction

The earliest reported study of the lanthanide oxidefluorides is attributed to Klemm and Klein[1], whose investigation revealed that the oxidefluorides have a cubic fluorite type lattice. Subsequently, Zachariasen[2] reported a rhombohedral structure for all oxidefluorides except those of Ce, Tm, Yb and Lu. This rhombohedral structure is now accepted as the correct room temperature phase[3] and the cubic phase found by Klemm and Klein is considered the high temperature modification. Both stoichiometric LnOF and slightly fluorine rich samples exhibit the cubic phase with the fluorine rich specimens retaining the cubic structure more readily upon cooling to room temperature. The transition temperature for the rhombohedral to cubic change (about 500°) is relatively cation independent.[4,5]

Other studies on the lanthanide oxidefluorides have shown regions of nonstoichiometry and solid solution in the composition range LnO_xF_{3-2x} in which $0 \leq x \leq 1$, and Ln = La, Nd, Sm, Eu, Gd, Er and Y.[3,6] The regions where $0.5 \leq x \leq 1$ appear to be distortions of the basic fluorite structure. In some cases (La, Y) a tetragonal distortion is evident[2], whereas in others[6] an orthorhombic distortion is observed. In either case, the distortion may be explained by occupancy of the tetrahedral holes present in the fluorite lattice by excess fluoride ions. The ability of fluoride ions to occupy these holes is further evidenced by the region of solid solution between europium oxidefluoride and europium trifluoride.[3]

A deta
lanthanide
prepare Eu_3
heating the
of starting
that the co
sesquioxide
600° and its
the Eu_2O_3 re
monoclinic t
in their phas

Work and
oxidefluoride

and reported a
neodymium oxid
reaction. Disc
oxidefluorides

In light o
on europium oxi
it appeared tha
lieu of Cataland
vaporization wor
since europium ha
the possibility o

A detailed study has not been made on the lanthanide sesquioxide-lanthanide oxidefluoride systems. Catalano and Bedford[3] attempted to prepare Eu_3O_4F by mixing stoichiometric amounts of Eu_2O_3 and EuOF and heating the mixture to 1600°. All attempts resulted in the retention of starting materials with no evidence of new phases. They concluded that the composition range between EuOF and Eu_2O_3 contained monoclinic sesquioxide at all temperatures and rhombohedral oxidefluoride below 600° and its cubic form above 600°. They add that in several experiments the Eu_2O_3 retained the low temperature cubic form above its normal monoclinic transition temperature, but did not include these results in their phase diagram.

Work and Eick[7] have studied the vaporization behavior of samarium oxidefluoride. They found the mode of vaporization to be:

$$3SmOF_{(s)} = Sm_2O_{3(s)} + SmF_{3(g)} \qquad (I-1)$$

and reported a $\Delta H°_{298}$ and $\Delta S°_{298}$ for this process. In a study of neodymium oxidefluoride, Shinn[4] observed a comparable decomposition reaction. Discussions on the decomposition of other lanthanide oxidefluorides cannot be found.

In light of the relatively small amount of information available on europium oxidefluoride and the previous vaporization study of SmOF, it appeared that a vaporization study of EuOF would be of interest. In lieu of Catalano and Bedford's discussion of the phase diagram and the vaporization work on SmOF, major difficulties were not anticipated, but since europium has the most stable divalent state of all the lanthanides, the possibility of $EuF_{2(g)}$ must be considered.

At the outset of this work, the vaporization of EuOF was considered a practice system in which to learn the various techniques in hopes of continuing the study to condensed EuF_2. As it turned out, EuOF became the whole project. Many interesting features of the system have been uncovered, but I have been unable to solve the complex EuOF-Eu_2O_3-EuF_3 system.

A. Vapori

1.

This

technique

If a

of molecul

z, may be r

where n is

velocity.[8]

the number

given by (I

where S_o is

The eff

the cosine d

placed coaxi

that part of

the target an

law over the

II. Theoretical Considerations

A. Vaporization

1. Technique and Theory

This vaporization study was carried out by the Knudsen effusion technique combined with target collection.

If a gaseous species is confined in a closed container, the number of molecules which strike a unit section of the container wall per unit time, z, may be represented by

$$z = n\bar{\nu}/4 \text{ molecules/cm}^2 \text{ sec} \tag{II-1}$$

where n is the total number of molecules and $\bar{\nu}$ is the average molecular velocity.[8] If an infinitely thin orifice is drilled into the container, the number of molecules which would escape through this orifice is given by (II-2)

$$N = S_o z \text{ molecules/volume} \tag{II-2}$$

where S_o is the area of the orifice.

The effusion of molecules through such an ideal orifice follows the cosine distribution law.[9] A circular target of radius, r, which is placed coaxially with the orifice at some distance, d, will collect that part of the molecules whose trajectory lies in the cone defined by the target and the orifice. By integrating the cosine distribution law over the volume represented by this cone, the fraction of the total effusate which strikes the target,

$$r^2/(d^2 + r^2) \qquad \text{(II-3)}$$

is obtained.

Finally, ideal gas behavior may be assumed for the vapor within the cell as long as conditions of molecular flow are obeyed (pressure less than 10^{-3} atmospheres).[8] When equations II-1 and II-3 and from kinetic theory $(8RT/\pi)^{1/2}$ for $\bar{\nu}$ are substituted into the ideal gas law, equation (II-4) is obtained.

$$P = [w/S_0t][2\pi RT/M]^{1/2}[(d^2 + r^2)/r^2] \qquad \text{(II-4)}$$

Conversion of all constants to give pressure in units of atmospheres yields equation (II-5)

$$P = 3.76 \times 10^{-4}\ w/S_0t\ [T/M]^{1/2}[(d^2 + r^2)/r^2] \qquad \text{(II-5)}$$

in which w represents the mass on the target expressed in grams, T, the temperature in degrees K, M, the molecular weight of the effusing species and t, the time in seconds during which a target is exposed to the beam.

2. Limitations of the Knudsen Technique.

a. Orifice Shape and Cell Geometry

A machined orifice cannot be made infinitely thin. For any orifice of finite thickness, L, some deviation from cosine distribution will occur since the molecules collide with the walls of the orifice and some may return into the container. This return of molecules causes the total effusate to be less than the theoretical amount and thus represents a lower pressure than that actually in the cell. Clausing[10] made a study of the effects caused by channel orifices and calculated for various orifice length to radius ratios, L/ρ, correction factors which compensate for the decreased amount of effusate. Pressure equation (II-5) with a Clausing correction, W_0, becomes

$$P = [3.76 \times 10^{-4}\ w/S_0 t]\ [T/M]^{1/2}[(d^2 + r^2)/r^2][1/W_0] \qquad \text{(II-6)}$$

A converging conical[11] orifice with a knife edge is a closer approximation to the ideal situation than is a channel orifice. If such a conical orifice is combined with a coaxial target of sufficiently small radius, r, that it collects 1% or less of the total effusate, the Clausing correction in equation (II-6) may be taken as unity[11] (cf. figure 1). The cone defined by the target and orifice (figure 1a) contains the same amount of effusate for either the ideal or non-ideal case since in this volume essentially only those molecules which travel in a straight line from the surface of the sample to the target are present. However, to calculate the total amount of effusate which would effuse if the cell orifice were ideal some correction factor must be applied. Freeman and Edwards[12] have computed the Clausing factors for converging conical orifices of various lengths, radii and conical angles.

b. Orifice Effects

To insure that the equilibrium within the cell is not disturbed to such an extent by the effusion that only a steady state, and not an equilibrium pressure is obtained, the diameter of the orifice must be at least ten times smaller than the mean free path of the gaseous species.[8] If the radius of the gaseous species is known, the mean free path may be calculated and the appropriate orifice selected. If such information is not known, the orifice size may be tested experimentally by repeating pressure measurements at the same temperature with markedly

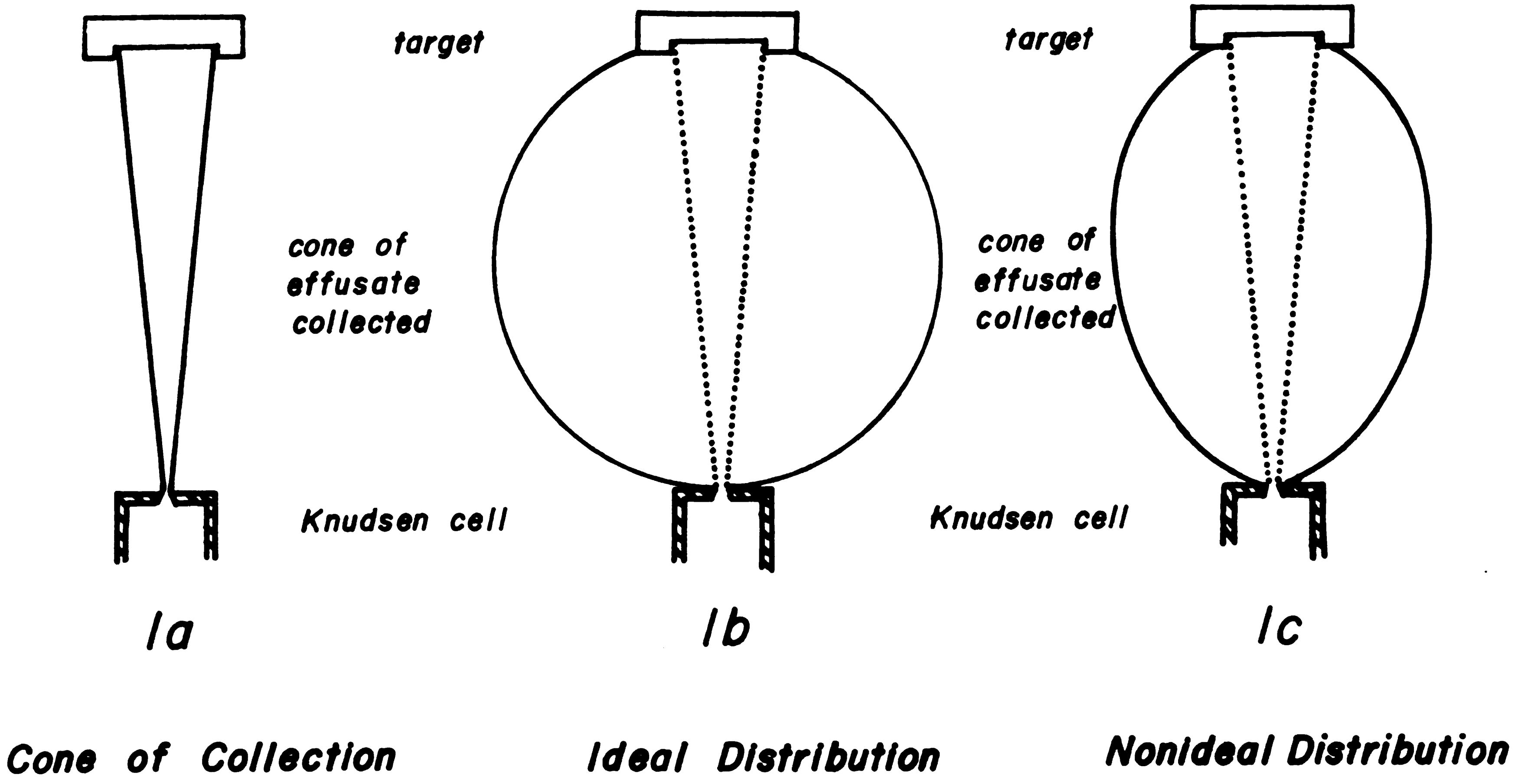

Figure 1. Distribution of Effusate.

differen

pressure

the orif

Meas

Since ver

some char

study[13] m

indicated

Other

the Knudse

One such c

a_e, may be

a vacuum a

sample.[14]

would be th

measurement

has shown t

the effecti

d.

Process

of the corre

processes pr

occur since a

evaporation a

constantly.

different sized orifices. If at the same temperature identical pressures are calculated for these different orifices, the sizes of the orifices are within the allowed limits.

Measurement of the orifice size takes place at room temperature. Since very high temperatures are reached in the course of an experiment some change in orifice area due to thermal expansion is expected. A study[13] made to determine the correction factor for such expansion indicated that this correction factor would be very close to unity.

c. Vaporization Coefficient

Other considerations which must be included in the limitations of the Knudsen technique do not directly concern the physical set up. One such consideration is the vaporization coefficient. This coefficient, a_e, may be defined as the ratio between the rate of vaporization into a vacuum and the rate at which an equilibrium vapor impinges on the sample.[14] The observable effect of a non-unity vaporization coefficient would be the absence of an equilibrium within the cell, and pressure measurements would be sensitive to orifice area variation. Rosenblatt[15] has shown that for finely divided samples, a_e is usually unity since the effective vaporization area is large.

d. Diffusion

Processes which are diffusion controlled may hinder establishment of the correct vapor pressure of a compound. Incongruent vaporization processes provide an excellent opportunity for diffusion limitations to occur since a new solid product is being formed in the course of an evaporation and thus the surface composition of the sample is changing constantly. Ackermann *et al.*[14] have calculated that most of the effusing molecules vaporize from the outermost atomic layer and therefore, the changing surface composition might be expected to interfere and to induce a diffusion controlled process.

Several experiments have been devised to ascertain whether or not the effects of diffusion are significant. One such test involves the use of samples of differing particle size in the course of several experiments. If a systematic trend of increasing measured pressure is found with more finely divided sample, diffusion may be occuring. A second approach is to follow the pressure as a function of time at constant temperature. In this case a drop in pressure with time indicates diffusion control of the evaporation. Yet another technique is to vary the temperature in different ways in the course of an experiment. For example, a series of targets would be collected with the temperature successively increased, then another series would be taken as the temperature was decreased through the same temperature range. If the measured pressures are lower for the series of targets where the temperature was decreased, diffusion may be present.

e. Sticking Coefficient.

Another error in pressure measurement may occur if the effusate does not adhere to the target. Liquid nitrogen is used to chill the target so that the energy of the striking molecule will be removed quickly, but in some instances this cooling may be inadequate. By placing a chilled disc with a hole in its center in front of the target, any molecules which pass through the hole in the disc and do not adhere to the target, but reflect from it should be trapped on the back of the disc. The amount of effusate collected on the back of the disc can then be measured and a correction factor calculated.

f. Interaction with Knudsen Cells.

Interaction between the sample and the materials from which the Knudsen cell is made should be avoided. Such an interaction causes the thermodynamic activity of the species involved to change. If the interaction can be accounted for, that is, if a chemical equation representing the reaction can be written, the effect of the interaction on the measured pressure may be predicted. For example, if an interaction is occuring between one of the gaseous species and the cell in an incongruent vaporization where two vapor species are present, the activity of the interacting molecule will be decreased. Since the equilibrium depends on the activity of both species, the activity of the non-interacting species will increase. The equilibrium constant has not changed, but if, as in the typical case, only one of the gaseous species is used to determine the vapor pressure, this calculated equilibrium constant will be in error.

B. Characterization of the Gaseous and Condensed Phases

Equation II-5 derived to determine the vapor pressure depends among other things on both the mass of the material collected on the target and on its molecular weight. Various methods such as total weight loss, torsion effusion, mass spectrometry, X-ray diffraction, and chemical analysis all yield information concerning the nature of the effusate.

1. Mass Spectrometry

Grimley[16] gives a detailed discussion of the use of mass spectrometry for characterization of the effusate. All ionic species present in the mass spectrum can be identified uniquely from the knowledge of the possible combinations of the various isotopes and their percent abundance. Determination of the neutral precursor for each ionic species is not simple. From a plot of ion intensity versus ionization energy, the appearance potential of the ions may be determined by extrapolation of the linear portion of the curve near the threshold to zero intensity (cf. figure 2). Appearance potentials of standards such as mercury or nitrogen must simultaneously be measured to determine the correction factor necessary to convert the ionization energy readings of the unknown to appearance potential values. Accurate values are obtained from this method only when the experimentally determined curves approximate that illustrated in figure 2.

The appearance potentials can be used to identify the neutral precursor, usually, by comparison to values obtained from related systems for which appearance potentials are known. In complex cases where similar systems have not been studied, additional information must be obtained by disturbing the equilibrium. By adding (or removing) certain compounds expected to comprise the effusate, the concentration of the other components in the effusate change. If this change in vapor concentration is followed through corresponding intensity changes of the various ionic species, the neutral precursor may become evident.

2. X-Ray Fluorescence

Once the vapor species has been established one may determine the total mass collected on a target during the vaporization process. In this study the amount of europium present on each target was determined by X-ray fluorescence. A full description of the fluorescence technique is reported elsewhere,[17,18] but figure 3 shows the basic

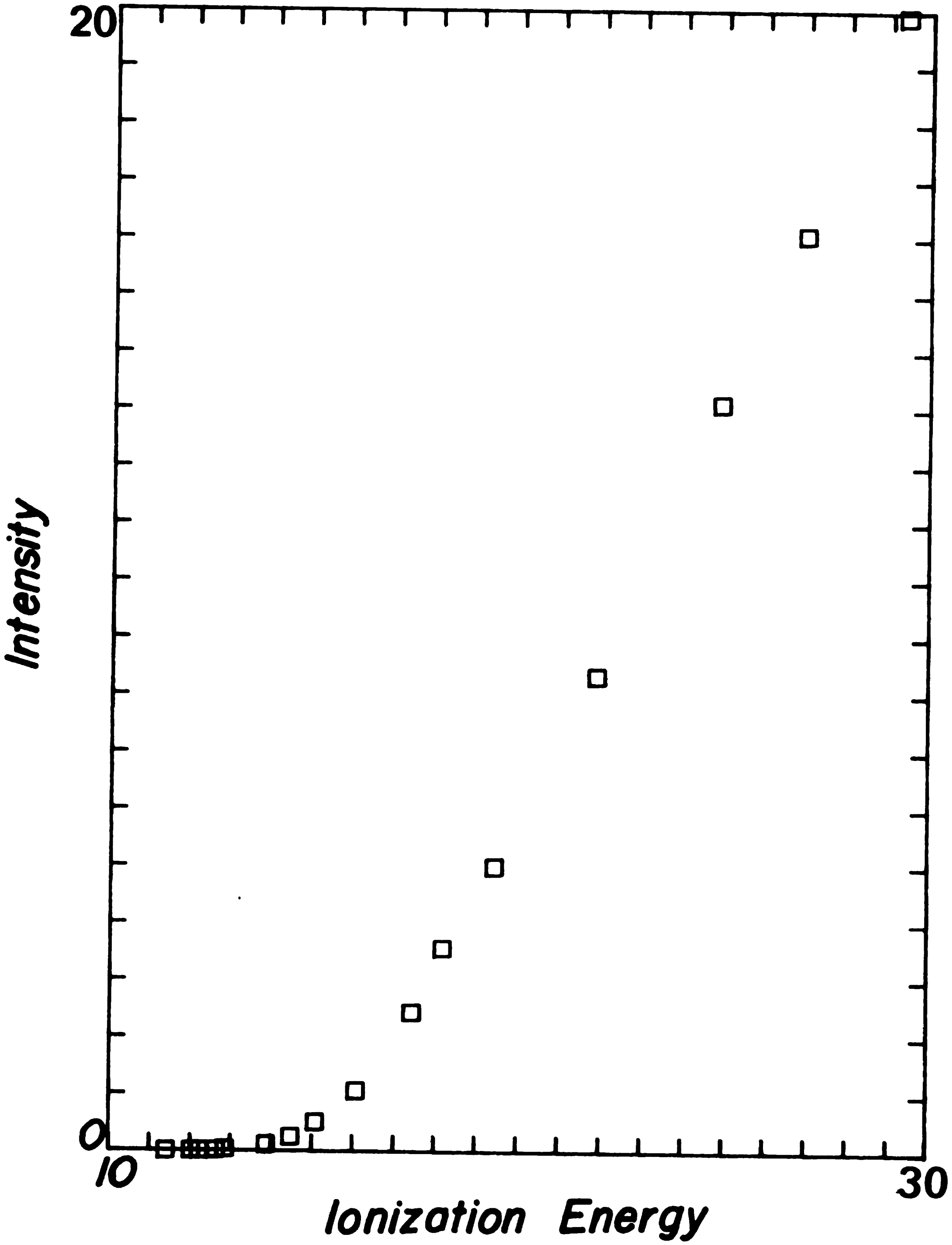

Figure 2. Appearance Potential Curve

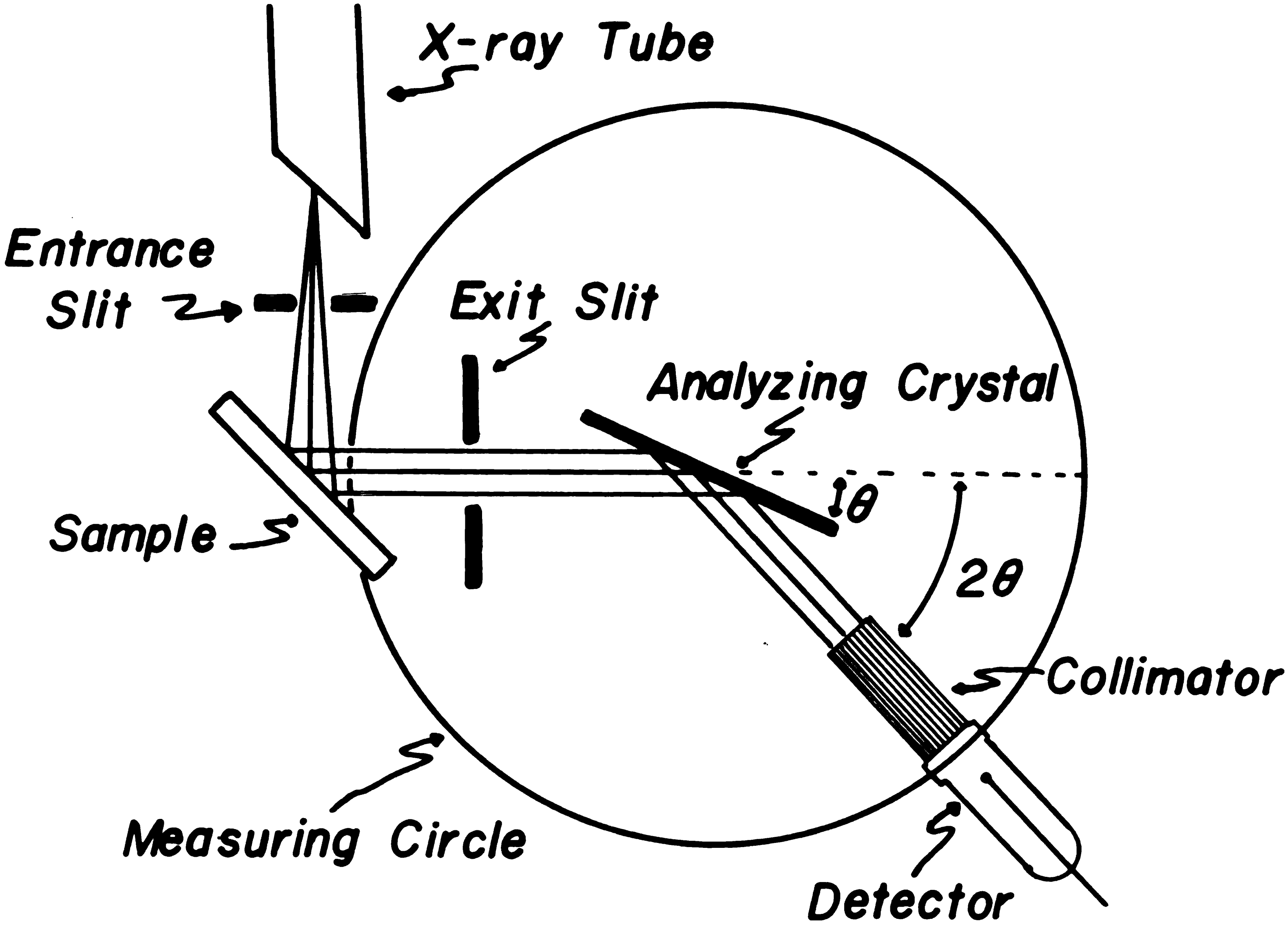

Figure 3. A Schematic of the X-Ray Fluorescence Spectrometer

features of the method. The X-ray tube emits radiation not only of the wavelengths characteristic of tungsten, but also of a broad continuous nature. This radiation strikes the target and excites electrons to higher energy levels and/or is deflected. Electrons which return to the ground state emit photons in the process of fluorescence. Electrons located near the nucleus are not affected greatly by the chemical environment and the energy they emit in going from an excited state to the ground state will be identical regardless of what compound they are in. Once the spectrometer has been optimized for a certain element, these conditions will apply for any compound containing that element. Detection of the fluorescence is accomplished by use of a single crystal. Bragg's equation which relates wavelength, λ, and hence energy, to interplanar distances is given as

$$n\lambda = 2d \sin\theta \tag{II-7}$$

Since a single crystal is used, that is, d is fixed, the energies may be detected by varying 2θ. Tables completed by Seivers[19] relate the various electron changes characteristic of an element to observed 2θ values for a graphite crystal.

C. Temperature Measurements and Corrections.

The Knudsen cell is designed so that temperature may be determined precisely with confidence. Since a target is situated above the orifice temperature measurement through the orifice is impossible during the course of the experiment. Therefore, an identical cavity is made in the bottom of the cell to replicate conditions of the top (cf. figure 4). This lower orifice is then assumed to be a black body hole from which any radiation emitted is characteristic of the temperature of the cavity.

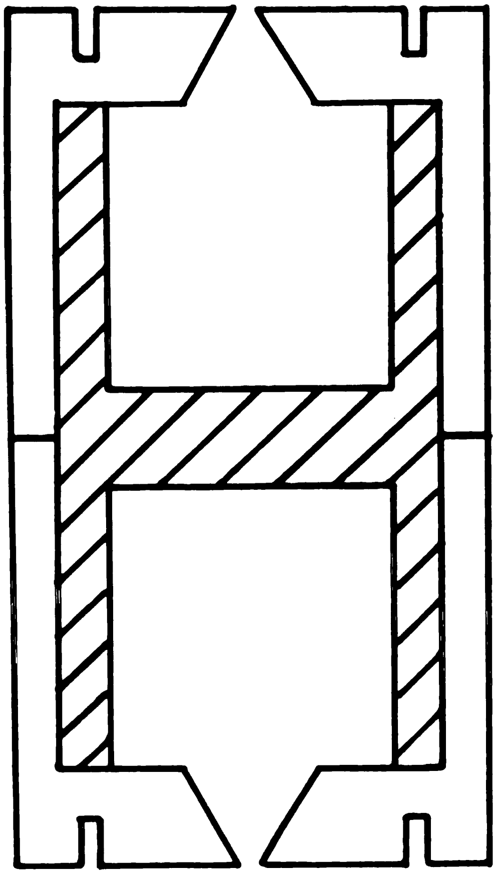

SYMMETRICAL EFFUSION CELL WITH SAMPLE AND OPTICAL CAVITIES

6/68

Figure 4. Symmetric Knudsen Cell

An optical pyrometer is placed at right angles with a prism which is located coaxially below the orifice through which the temperature is to be read. According to Margrave,[20] the radiation which is absorbed by both the prism and the glass of the vacuum line may be accounted for by application of Wein's and Beer's Laws (II-8)

$$(1/T_{obs.} - 1/T_{act.}) = \text{an empirical constant} \qquad \text{(II-8)}$$

A 3 mm wide band filament lamp is used to determine the Wein's Law constant by first reading the temperature of the filament and then rereading it through the prism and glass base of the vacuum line. Calibration data for each pyrometer have been furnished by the National Bureau of Standards for the temperature range of 800° to 2000° in accordance with the 1948 International Practical Temperature scale and are used to convert the pyrometer readings to the actual observed temperature before the absorption correction factor is applied.

D. Phase Relationships

1. Possible Composition Range for EuOF-Eu_2O_3

No known compounds or regions of nonstoichiometry have been reported at room temperature between the compositions Eu_2O_3 and EuOF[3], but such observations do not preclude the existence of either at high temperatures. Indeed, the general formula, $EuO_{1+x}F_{1-2x}$, where $0 \leq x \leq 0.5$, would include all possibilities. Previously unreported compounds which exist at temperatures over 1200° would become evident in the course of a vaporization study, since the equilibrium pressures will change as new equilibria are established. Knowledge of the correlation between Gibb's phase rule and vaporization behavior will help to clarify this point.

2. Phase Rule

The degrees of freedom, F, which exist for a particular system may be ascertained from the phase rule,

$$F = C - P + 2 \tag{II-9}$$

where P is the number of phases present at equilibrium and C represents the number of components, the smallest number of independently variable constituents needed to define the composition of all phases.[21] Possible degrees of freedom are the variables temperature, pressure, and composition. With this definition in mind one is able to investigate the various possibilities which exist in a vaporization study.

3. Modes of Vaporization and Their Relation to the Phase Rule

There are two modes of vaporization, congruent and incongruent. A substance that vaporizes without changing its chemical composition undergoes congruent vaporization. Since there are only two phases, one condensed and one gaseous, and only one component by definition of congruency, there will be only one degree of freedom. In other words, fixing the temperature automatically sets the pressure once equilibrium is established or vice versa.

In an incongruent vaporization the starting material decomposes to a new solid product and a gaseous phase of composition different from that of the solids. For most ternary systems which undergo incongruent vaporization there will be one gaseous and two solid phases, or $P = 3$. If an equation relating all constituents at equilibrium can be written, $C = 2$ and F is unity. Experimentally this fact is evident when a plot of ℓnP versus $1/T$ yields a straight line.

In a comparable ternary case in which P = 3, and C = 3, two degrees of freedom exist. Composition along with temperature or temperature along with pressure must be fixed to yield a unique pressure or composition, respectively.

Still another possibility in an incongruent vaporization is the existence of a solid solution which forms at high temperatures. For a ternary system formation of this solution would decrease P from three to two. Two degrees of freedom would exist when C equals two. If composition could not be fixed in the course of a vaporization experiment, a plot of ℓnP versus 1/T would not necessarily yield a straight line and, in fact, shouldn't. To obtain any meaningful thermodynamic data under these conditions one of the variables must be held constant. From an experimental viewpoint, it is easier to hold the temperature constant and to investigate the relationship between pressure and composition than to hold composition constant. If, as the phase rule indicates, there are only two degrees of freedom, a linear relationship will exist between ℓnP and 1/T for each composition.

It was stated earlier that application of the phase rule was helpful in obtaining a phase diagram for a system. In actuality, the experimental results of the vaporization experiments allow deduction of the numbers of degrees of freedom. One can work backwards to decide what phases and components are affecting the equilibrium. For example, consider a ternary system (C = 2) which yields at constant temperature a plot of pressure versus time which decreases initially, then levels out, and finally drops again. For the horizontal region, dP/dC = 0, F must equal 1, therefore P = 3 or two solids and one gaseous phase are in equilibrium. For the regions where pressure is decreasing there must be more than one degree of freedom; that is, the composition must be varying. Such a situation is indicative of solid solution formation. Figure 5 represents a phase diagram which is consistent with these data.

E. Thermodynamic Calculations

1. General Considerations

As I have stated in the previous section, a linear relationship is usually found between ℓnP and $1/T$ when there is only one degree of freedom in the system. From such a linear relationship one can derive values for the vaporization process by use of equations (II-10) and (II-11) on the assumption that the heat capacity change for the

$$\Delta G^\circ = -RT\ell nK \qquad \text{(II-10)}$$

$$-\ell nK_T = (1/T)\ (\Delta H^\circ_T/R) - \Delta S^\circ_T/R \qquad \text{(II-11)}$$

vaporization process is constant over the temperature range of the study. If the heat capacity change is not constant, its variability must be considered in the equations.

The ΔH° and ΔS° values determined from the slope and intercept of the linear plot are considered the enthalpy and entropy changes, respectively, for the vaporization process at the mean temperature of the study. Through thermochemical cycles these values from the slope and intercept must be reduced to standard temperature by use of heat capacity data. Such a data reduction is known as the "second law" approach and is described in detail by Haschke.[22]

These ΔX°_{298} values provide information on the relative stability of the components of the reaction and allow for comparison to other reactions.

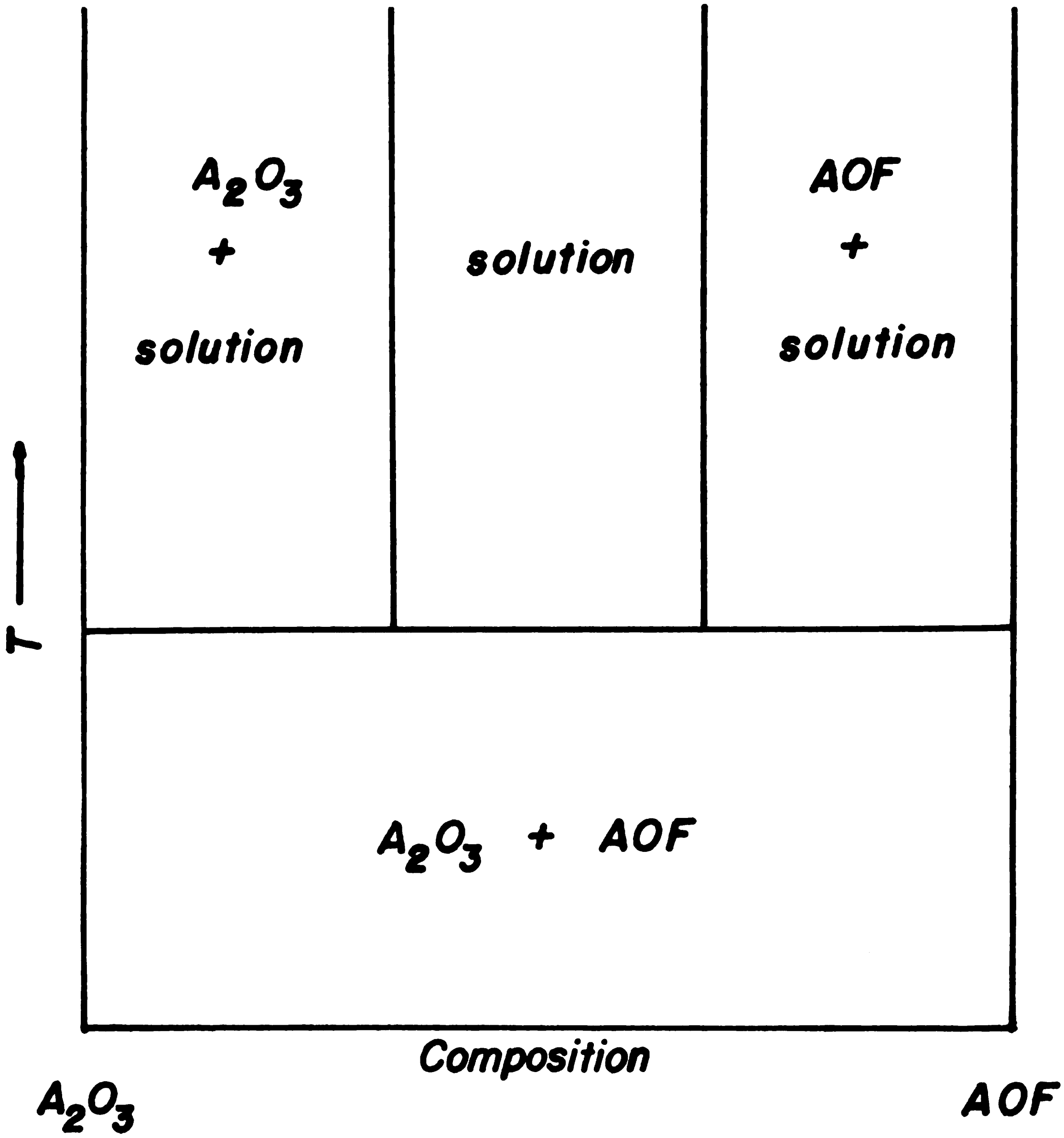

Figure 5. Hypothetical Phase Diagram

Another approach to data reduction is the "third law method" in which either derived or estimated free energy functions are used in the calculations in conjunction with the ℓnK values experimentally determined from each data point. The third law technique is generally more applicable since a linear relationship between ℓnP and $1/T$ need not always be established before meaningful thermodynamic values can be obtained. In a situation where there is formation of a solid solution so that composition is changing constantly as vaporization proceeds, it is theoretically possible to establish the ℓnP to $1/T$ relationship for each composition. Experimentally this task is extremely difficult. Each target represents the average pressure of some average composition during the collection time period. It is most difficult to repeat experiments so that successive pressure measurements represent identical average compositions. Extrapolation procedures can be used to determine the pressure at each composition, but the extrapolation introduces more uncertainty in the final values. Only one assumption, that enthalpies of formation vary only slightly with changing composition, needs to be made to use the third law to obtain ΔH°_{298} values. For a discussion of this method, the reader is referred to Haschke's dissertation.[22]

A final approach to data reduction involves calculation of the activity of one component in a solid solution by determining the ratio of the pressure of that component in the vapor to its standard pressure at the same temperature.

2. Third Law Calculations

The third law method employs the free energy function, fef, as a means of obtaining a ΔH°_{298} value for each data point. The free energy function is represented by equation (II-12) or (II-13)

$$\text{fef} = (G^\circ_T - H^\circ_{298})/T \qquad \text{(II-12)}$$

$$\text{fef} = (H^\circ_T - H^\circ_{298})/T - (S^\circ_T - S^\circ_{298}) - S^\circ_{298} \qquad \text{(II-13)}$$

The change in free energy function, Δfef, may be calculated from the values of fef for each product and reactant by equation (II-14) where ν represents the stoichiometric coefficients and i and j represent products and reactants, respectively.

$$\Delta\text{fef} = \sum_i \nu_i \text{fef}_i - \sum_i \nu_j \text{fef}_j \qquad \text{(II-14)}$$

The free energy functions of many compounds have been tabulated and for those not tabulated fef may be readily calculated from equation (II-13). The necessary enthalpy, entropy and standard entropy values may also be approximated (_cf._ II E, 3).

Free energy functions form smooth curves when they are plotted against temperature and therefore allow interpolation.[23] Variation of composition may also be incorporated into the fef by interpolating values from a plot of fef versus composition, provided several points are known or may be estimated to establish the curve.

Once a Δfef has been determined for a characterized reaction at temperature intervals, the calculation of ΔH°_{298} values proceeds in a straightforward manner through equation (II-15),

$$\Delta\text{fef} = (\Delta G^\circ_H - \Delta H^\circ_{298})/T \qquad \text{(II-15)}$$

or through use of equation (II-16) obtained by substitution of equation (II-10) into (II-15).

$$\Delta H^\circ_{298} = -(\Delta fef + R\ell nK_T)T \qquad \text{(II-16)}$$

Alternatively, if ΔH°_{298} and Δfef are known, ℓnK can be calculated at selected temperatures to check hypothetical equilibria.

3. Calculation and Estimation of Thermal Functions

In many cases, thermal data have not been determined for lanthanide compounds, or if they are available they do not cover the temperature range of interest. However, a statistical thermodynamic approach can be taken to obtain the appropriate free energy functions if a vibrational study has been made on the gaseous molecules. For solids, Kopp's Rule[23] may be applied to determine the heat capacity for temperatures greater than 298 K.

a. Free Energy Functions from Vibrational Data

Thermal functions of a compound can be divided into the translational, rotational, vibrational and electronic components. By use of the partition function the amount of energy contributed by each of these components may be calculated. A detailed discussion of the mathematics involved in deriving the entropy by use of the partition function can be found in most Physical Chemistry texts. However, a few of the more important features of the equation will be pointed out here.[24]

Since the energy level distribution is not known, the assumption is made that the molecule is in its ground state, thus for the electronic contribution, S_{elec}, is given as $R\ell ng_0$ where g_0 is the ground state multiplicity. From previous studies[25,26] the statistical weight of g_0 is taken as 16 and 14 for EuF_2 and EuF_3, respectively.

The symmetry of the molecule must also be considered in calculating $S°_T$ and the term $R\ell n\sigma$ accomplishes this. For europium difluoride, σ is taken as two and for europium trifluoride, $\sigma = 3$.

For the rotational contribution, the moment of inertia must be known. Again, many texts give equations for determining the moments of inertia for molecules of any shape. This study relied on the equations given by Moelwyn-Hughes.[27] If either internal free or restricted rotation occurs in the molecule, further adaptation must be made to the rotational contribution.

Vibrational contributions to the entropy depend on the fundamental vibrational energy levels of the gas. These must be experimentally determined since comparison with similar molecules does not always prove valid.

As in the case of entropy, heat capacity and (H_T-H_0) values may be calculated if the structure and vibrational levels are known. The same assumptions that the molecule is in its ground state electronic configuration and has no internal free or restricted rotation must be applied to validate equations (II-17) and (II-18) which are used for non-linear molecules.[28]

$$Cp = 4R + \sum_{i=1}^{3n-6} R(h\nu_i/kT)^2[e^{h\nu_i/kT}/(e^{h\nu_i/kT} - 1)^2] \qquad \text{(II-17)}$$

$$(H°_T - H°_0) = 4RT + \sum_{i=1}^{3n-6} [Nh\nu_i/(e^{h\nu_i/kT} - 1)] \qquad \text{(II-18)}$$

h = Planck's constant

k = Boltzman's constant

ν = Vibrational energies

N = Avogadro's number

b. Estimation of Heat Capacities for Solids

To obtain thermal data at various temperatures, the heat capacity of some compounds must be estimated. For high temperatures, Kopp[23] has determined that each atom of a solid contributes 3R to the heat capacity. The following equations[22] can be used to estimate the heat capacity of a binary or ternary system if the heat capacity of another binary system with the same heavy element is known.

$$Cp\ (A_xB_y) = [x/u]\ [Cp(A_uB_v)] + [(uy - vx)/2]\ [3R] \qquad \text{(II-19)}$$

$$Cp\ (A_xB_yC_z) = [x/u]\ [Cp(A_uB_v)] + [(uy - vx)/2 + z]\ [3R] \qquad \text{(II-20)}$$

The symbol A represents the heaviest element and the two compounds must have similar ionic character.

c. Approximation of Standard Entropies of Solids

Latimer[29] measured the entropies of many solids and concluded that each element makes a specific contribution to the entropy for each oxidation state, regardless of the compound in which the element is bonded. Westrum[30] extended Latimer's study to the rare earth oxides and developed a set of lattice contributions specific to these elements. He also estimated the magnetic contribution for each lanthanide. By combining Latimer's and Westrum's work, the following equation may be used to estimate the entropy of lanthanide solids.

$$S°_{298} = \sum_i x_i S°_i + \sum_i x_i M_i \qquad \text{(II-21)}$$

M_i = magnetic contribution

x_i = subscript in the molecular formula

III. Experimental

A. Equipment

1. Target Collection

The apparatus used is basically the unit designed by Kent[13] with the following two exceptions. 1. A copper plate has replaced the quartz shutter. 2. The collimator is no longer used to determine the angle that the target subtends. Instead, the area of the target seen by the X-ray fluorescence beam and consequently the solid collection angle is limited by a 45° beveled copper insert placed in the target.

2. X-Ray Fluorescence Equipment

The instrumentation used in quantitatively analyzing the collected effusate was a Norelco Vacuum fluorescence spectrometer equipped with a graphite analyzing crystal, a tungsten tube powered by a Norelco XRG 5000 generator, and a Harshaw NaI(Tl) scintillation detector and associated electronics.

3. X-Ray Diffraction

An 80 mm radius Haegg-type focussing vacuum X-ray diffraction camera[31] was employed to give crystallographic analyses of powdered samples. Radiation emitted by a copper X-ray tube powered by a Picker generator is diffracted from a quartz crystal to obtain the K_α component. This component is directed through the powdered sample and diffracted by it.

4. Temperature Measurement

National Bureau of Standards calibrated Leeds and Northrup disappearing filament-type optical pyrometers (serial numbers 1619073, 1524388, and 1572579) were used to determine the temperature of the Knudsen cell. For other experiments where knowledge of the temperature was necessary, either a platinum platinum-10% rhodium thermocouple with a Honeywell potentiometer (model 27-20) or a chromel alumel thermocouple with a Sym-Ply-Trol meter was used.

5. High Temperature Mass Spectrometry

a. Spectrometer

Investigation of the effusate was accomplished with the Model 12-107, Bendix Time-of-Flight instrument which together with the associated heating circuits has been described by Pilato.[32]

b. Mass Spectrometer Cells

All studies performed in the mass spectrometer were effected in molybdenum effusion cells of the design prescribed by Pilato.[32]

6. Micrograph

A Bausch and Lomb Dynazoom micrograph fitted with a Polaroid 4 x 5 Land Camera attachment was used to photograph the cell orifice, which was illuminated by a hi-intensity external light source.

7. Heating Apparatus

Heating of the effusion cells was accomplished by a 20 KVA Thermonic 200-400 KHz induction generator. Additional heating, especially that required for cell outgassing and for some preparative work, was carried out in a high speed vacuum line fitted with a current concentrator and powered by another similar induction generator.

Laboratory tube furnaces and a Marshall Products Co. platinum-40% rhodium wound tube furnace were also employed.

B. Preparative

1. Europium Oxidefluoride

All preparations of europium oxidefluoride involved the general method[1] of mixing stoichiometric amounts of europium trifluoride and either the monoclinic or cubic form of europium sesquioxide, and heating the resulting mixture to 600° in a horizontal tube furnace for several hours. Platinum boats were used to contain the reactants in a Vycor tube through which helium previously dried through a P_2O_5 tower and a liquid nitrogen chilled trap flowed continuously during the heating process. All reactants and products were handled in air and stored in dessicators.

a. Europium Sesquioxide

Europium sesquioxide (99.9% pure, Michigan Chemical Corp.) was calcined in a muffle furnace at 900° to remove absorbed gases. The body-centered cubic form resulted from this heating. To obtain the monoclinic form the sesquioxide was heated to above 1200°. The monoclinic phase does not readily convert to the cubic form when it is cooled. Since the calcining of a sample may decrease surface area and hence its activity, very finely divided sesquioxide was prepared by thermal decomposition of europium oxalate at 400° in air.

b. Europium Trifluoride

Two methods[33] were used for the preparation of europium trifluoride. The first involved the mixing of europium sesquioxide with a ten-fold excess of ammonium bifluoride. The NH_4HF_2 was made by dissolving

NH_4F (Baker Analyzed Reagent) in 48% hydrofluoric acid (Allied Chemical) and boiling off the excess water. A platinum boat which was situated in a Vycor tube contained the mixture while it was heated to 300° for ten hours under a flow of helium.

The other method involved the precipitation of europium trifluoride hydrate and subsequent removal of the waters of hydration. Europium sesquioxide was dissolved in hydrochloric acid and then filtered to remove any insoluble residue. Addition of 48% HF reagent to the filtered solution caused precipitation of the trifluoride hydrate which was then centrifuged and decanted. After several washings with dilute HF and subsequently with ethanol, the trifluoride was confined in a platinum boat and was dried at 110° for several hours. The dried material mixed with a 6:1 mole excess of NH_4F and was then placed in a tube furnace and heated to 600° for 4 hours.

C. Analysis

1. Powder X-Ray Diffraction Techniques

The general technique of sample preparation and film measurement for a Guinier camera is given by Stezowski.[31] Powdered platinum was used as the internal standard. The diffraction data were reduced with the aid of a least squares program written by Seivers for a Hewlett-Packard 9100B calculator and the program ANIFAC written by Larson, Roof, and Cromer.[35] This latter program which was run on a CDC 3600 computer calculates from known atomic positions, scattering factors and estimated thermal parameters, the intensity and $\sin^2\theta$ values for each reflection. An absorption coefficient was estimated. In most cases published structural data were used for comparison.

2. Chemical Analysis

a. Europium

Europium analysis was accomplished by weight change upon conversion of the sample to the sesquioxide. Weighed samples were placed in platinum crucibles which had been heated to constant weight. These crucibles were in turn placed in a Vycor tube and were heated to 950° for 3 to 6 hours, depending on the size of the sample. A flow of oxygen, which was saturated with moisture by bubbling it through water, was maintained through the tube.

b. Fluorine

The amount of fluoride present in Knudsen cell residues was determined by difference from a knowledge of the composition and total mass of the effusate and the composition of the starting material. To confirm this difference determination the HF produced by the stream of moist oxygen described above was bubbled through a dilute sodium hydroxide solution. This solution was then analyzed for fluoride content by a method devised by Megregian.[36] In this procedure the bleaching of a zirconium eriochrome cyanine R complex by the fluoride ion is measured quantitatively with a spectrophotometer.

Standard fluoride solutions were prepared from NaF within the range of 0 to 70 μg $\bar{F}$/50 ml of solution. A 5 ml sample of zirconium reagent and 5 ml of the eriochrome cyanine R solution were added to the 50 ml aliquots and then absorbance readings were taken at 527.5 mμ on a Cary 14 spectrophotometer. The sodium hydroxide solutions were treated in the same manner and concentrations were calculated from the least squares fit of the absorbance readings of the standard.

c. Oxygen

No direct tests were made for oxygen content.

D. Vaporization Techniques

1. Target Collection Method

a. General Procedures Followed for all Experiments

Outgassed Knudsen cells of the design shown in figure 4 were supported within a glass vacuum line (cf. figure 6). Coaxially above the cell, ten to twelve copper targets were suspended in a metal magazine which was cooled with liquid nitrogen. The target-orifice distance was measured with a cathetometer (Gaertner Scientific Co.). The cell was heated by induction once the vacuum within the line had decreased to 10^{-6} torr. Temperature was increased at a rate such that the vacuum remained below 10^{-4} torr. When the same temperature could be read successively, a state of equilibrium was assumed and a target was exposed for the time period calculated from data collected in an initial experiment. This time period was recorded on a laboratory timer (Lab Chron) and varied between 2 and 120 minutes. The target was then ejected and the next fell into place. In cases where long times of collection were required a Latronics ColoRatio Pyrometer and a Leeds and Northrup temperature controller were used to control the temperature which was determined by optical pyrometry.

At the conclusion of a few vaporization experiments the target magazine was replaced with an optical window and the temperature of the upper orifice was compared with that of the lower orifice. Coil position was also changed to determine its effect on the temperature of the upper and lower halves of the cell.

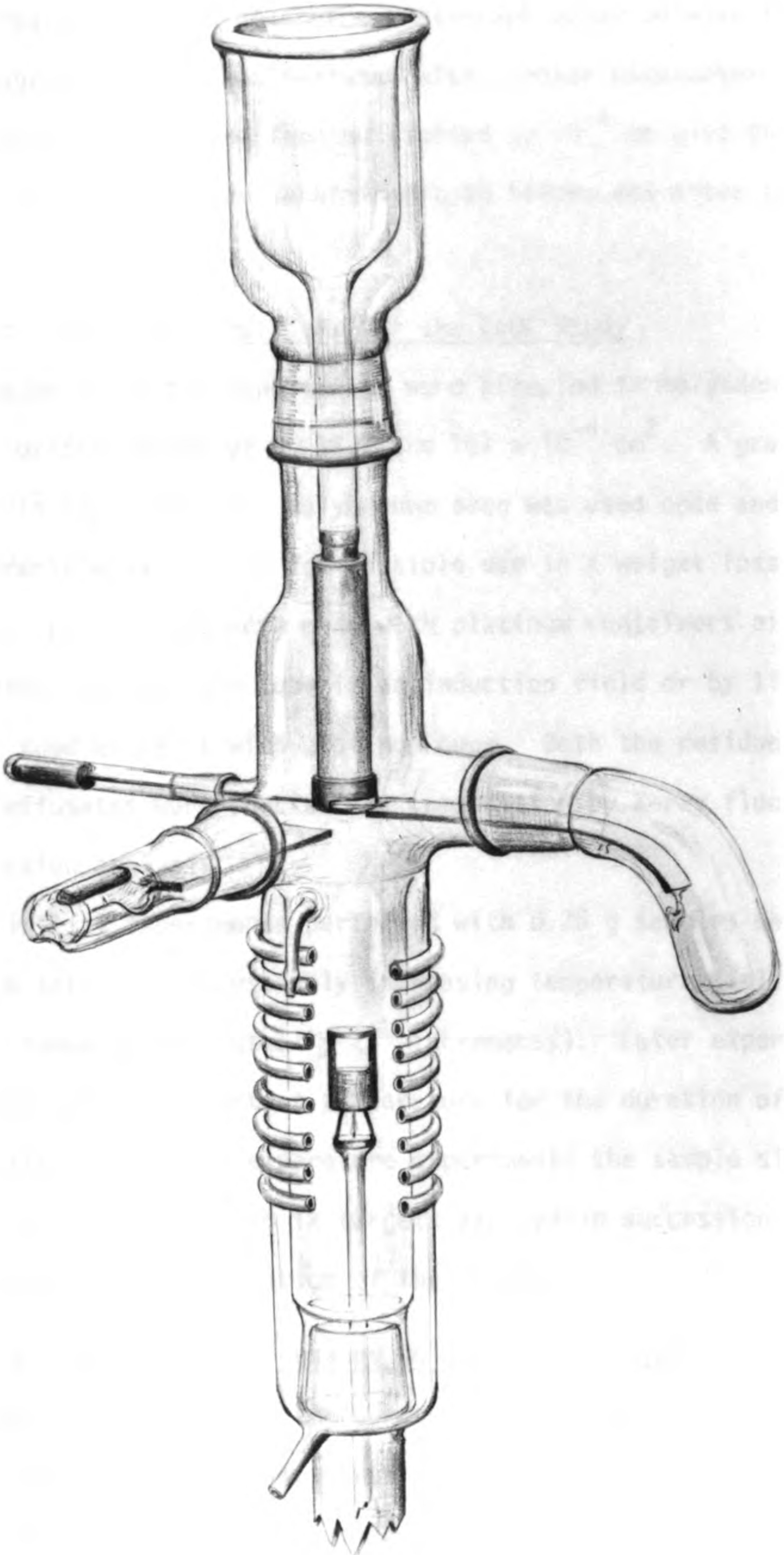

Figure 6. Vaporization Apparatus

b. Measurement of Orifice Area

The area of the orifice in the photograph obtained with the bench micrograph (100 X) was measured with a polar planimeter (Keuffel and Esser Co.) and then multiplied by 10^{-4} to give the real area. The orifice area was determined both before and after each experiment.

c. Specific Conditions for the EuOF Study

The majority of the experiments were effected in molybdenum cells with orifice areas of 9, 38.2 and 101 x 10^{-4} cm^2. A graphite cell with a thoria cup liner in a molybdenum oven was used once and a tungsten crucible was tested for possible use in a weight loss experiment. Later tests were made with platinum containers either by suspending the platinum tube in an induction field or by lining molybdenum Knudsen cells with platinum cups. Both the residues and collected effusates were checked for composition by X-ray fluorescence and diffraction analysis.

From initial experiments performed with 0.25 g samples data points were taken at successively increasing temperatures followed by decreasing temperatures (usually 25° increments). Later experiments were carried out at a constant temperature for the duration of the run. For these constant temperature experiments the sample size (0.05 g) was such that 10 to 12 targets exposed in succession would represent complete decomposition of the sample.

d. Analysis of Effusates Collected on Targets

The mass of europium in the compound deposited on the target during a vaporization experiment was determined by X-ray fluorescence. The fluorescence unit had been optimized for detection of europium by previous investigators in the course of their studies of europium compounds. Optimization procedures are discussed by Haschke.[22]

The $L\alpha_1$ energy level was followed by scanning its general region and selecting the 2θ value at which the peak maximized. This procedure was repeated at the beginning of each counting session.

A standard curve of counts versus micrograms of europium was obtained by counting targets which had deposited on them weighed amounts of solutions of known concentration of europium. These solutions were made by dissolving europium sesquioxide in HCl and then boiling off much of the acid. The solution was then diluted with distilled water in volumetric flasks. The most reproducible results for obtaining a value of counts per microgram occur when the solution is placed on the target in many tiny drops rather than a few large ones. This procedure gives a more uniform coating and decreases self-absorption in the spectrometer.

Each group of targets to be used in a vaporization experiment was handled in the following fashion: Targets were cleaned in concentrated hydrochloric acid. The collection surface was scraped with fine sandpapper. The cleaned blank targets were then scanned to obtain a background correction. One blank target was kept as a standard and counted several times during each use of the fluorescence unit. Use of this blank target permitted correlation of background intensity from day to day. After a vaporization the targets were again counted along with the standard blank and a target with known mass of europium deposited on it so that variations in the counts/μg could be taken into consideration.

E

i

(

1

f

(

c

t

F

t

l

in

ef

le

by

exp

evi

the

ca.

E. Characterization of the Mode

1. Effusate

a. Collection

The effusate of an europium oxidefluoride vaporization was collected in an inverted quartz cup which was supported over a Knudsen cell. Collection temperatures were near the extremes of the range 1100-1500°. The effusate was scraped from the cup and an X-ray diffraction pattern taken of it.

b. Weight Loss

A tungsten Knudsen cell heated to constant weight was loaded with 0.25 g of europium oxidefluoride and heated under vacuum again until constant weight was achieved. Guinier diffraction pictures were taken of the residue.

c. Mass Spectrometry

Three different experiments were carried out in the mass spectrometer. For all three, the system was pumped to a pressure of 10^{-6} torr after the sample had been loaded. The cells were allowed to outgas below 1000° to ensure no loss of effusate. The temperature was then increased as rapidly as possible so that the initial rapid rate of effusion could be detected. The background pressure was maintained less than 10^{-6} torr. Background scans were taken at various temperatures by shuttering the cell effusate from the ionizing beam. In the initial experiment the temperature at which effusate species were first evident was established. The ion intensity of the EuF^+ peaks was then monitored as a function of time at constant temperature with a *ca*. 50 ev ionization energy until most of the sample had been depleted.

This same procedure was repeated in the second experiment. Appearance potential data were obtained for all evident europium-containing peaks, except Eu^+, by measuring the ion intensity while the ionization energy was decreased from 30 to *ca*. 8 ev. The appearance potentials of both mercury and nitrogen were taken to calibrate the ionization energy scale. The temperature range of the various mass spectrometric investigations was 1200-1500°.

2. Residue

The residue of each vaporization experiment was subject to X-ray diffraction analysis. The diffraction data were examined for the presence of equilibrium phases and for changes in interplanar d-spacing or their relative intensities. In some cases chemical analysis was performed on the residue.

Attempts to prepare phases seen in the diffraction patterns of the residue were accomplished by sealing various mixtures of Eu_2O_3 and EuOF in quartz tubes under a partial pressure of helium. At first no container was used, but later the mixture was enclosed in a platinum capsule before being placed in the quartz ampoule. These samples were heated to temperatures between 800° and 1200° in the Marshall furnace for varying lengths of time. The ampoules were removed from the furnace and immediately placed in cold water in hope of quenching a high temperature phase. The cooled samples were then examined by X-ray diffraction.

3. Use of X-Ray Fluorescence to Detect Impurities or Secondary Reactions

Standard targets were made by placing small quantities of the material of interest on the target with Scotch tape. Various 2θ

regions reported to be characteristic of the radiation emitted by such elements as molybdenum, thorium, and platinum were scanned and compared with the background evidenced by blank targets to find the best region for detection. A powdered sample which was to be analyzed for one of these elements was placed on a copper target with Scotch tape and the selected 2θ region was scanned again.

4. Reaction of EuF_3 with Different Cell Materials

Europium trifluoride was heated in both molybdenum and platinum crucibles under a vacuum in the susceptor line to *ca*. 1450° to check for reaction with the cell. A Vycor cup was placed above the molybdenum cell so that the effusate could be collected. The platinum cell was fashioned in such a manner that only the bottom part containing the EuF_3 was heated by the susceptor. The rest of the crucible was located out of the field so that it remained at a much lower temperature and the effusate could condense there.

IV. Results

A. Results of Preparative Techniques

1. Europium Trifluoride

Composition of the trifluoride prepared by dehydration of the precipitated trifluoride hydrate was confirmed by X-ray diffraction (*cf.* IV-B-1).

2. Europium Oxidefluoride

All preparative attempts yielded the oxidefluoride, but all except one sample still contained some cubic europium sesquioxide. This one exception which was the product of the mixture of EuF_3 and monoclinic Eu_2O_3 appeared as pure rhombohedral oxidefluoride in the X-ray diffraction pattern.

B. Analytical Results

1. X-Ray Diffraction

Phase purity of a sample was determined by matching the position and intensity of each diffraction pattern line with the values produced by the program ANIFAC (*cf.* III-C-1). For these calculations the lattice parameters and atomic positions of EuF_3,[37] EuOF (rhombohedral);[2,38] C-Eu_2O_3[39] and B-Eu_2O_3[40] reported by previous workers were used. Isotropic thermal parameters contained in this program were used for every compound except B-Eu_2O_3, for which the reported values were substituted. An absorption coefficient of unity was assumed. The only impurity lines found in the rhombohedral oxidefluoride were those of C-Eu_2O_3. The observed and calculated $\sin^2\theta$ values are listed in Appendix I.

2. Chemical Analysis

Well annealed cubic sesquioxide X-ray diffraction patterns were obtained after pyrohydrolysis of the oxidefluoride samples. Weight loss data are given in Table I.

Table I. Weight Loss Data and Percent Europium

Sample	% Weight Loss	% $\frac{EuOF}{Eu_2O_3 + EuOF}$	% Eu
Prep III	106.9 ± 0.8	excess F	80.9 ± 0.5
	97.5 ± 0.8	97.39	81.4 ± 0.5
Prep IV	106.2 ± 0.8	excess F	81.2 ± 0.5
	103.4 ± 0.8	excess F	81.1 ± 0.5
Theoretical	-	-	81.28

Several attempts to collect the hydrogen fluoride produced from passage of the moist oxygen over commercial NaF samples at 800° proved unsuccessful. Even after the apparatus had been compacted to minimize the distance the HF gas had to travel and in which it could contact the glass apparatus only 78% collection of the fluoride liberated was obtained in the best results. Besides not collecting all the fluoride, it was difficult to reproduce the rate of oxygen flow from run to run. Therefore fluorine analysis was not effected.

C. Results of X-Ray Fluorescence Calibration

A set of copper targets with a varying number of micrograms of europium was prepared by this researcher and a standard of 2407 ± 50 counts/microgram established. This number was within the standard deviation of the 2442 ± 50 counts/μg found by A. V. Hariharan, a co-worker studying $EuCl_2$. Excess acid in my standard solutions caused some attack on the copper target and on repeated use of the target loss of europium occurred. Therefore, the standard prepared by Hariharan was used for the duration of the research.

D. Vaporization Results

1. Mode of Vaporization

a. Effusate

Collection of the effusate of europium oxidefluoride confined in a molybdenum crucible resulted in a thin brown film on the collection cup at both 1100° and 1500°. The diffraction pattern of both collections exhibited diffuse lines which fit an fcc cubic pattern ($a = 5.78 \pm 0.01$ Å). The pattern of the sample collected at 1500° also contained an extra line which did not fit the cubic indexing.

The results obtained from mass spectrometry are presented in Table II and Figures 7 and 8.

No peaks corresponding to EuF_3 could be found by scanning in the temperature range 1290° to 1500° and by varying the ionization potential from 15 ev to 30 ev.

The 19 and 38 mass unit regions were scanned in attempts to identify F^+ or F_2^+, but the normally high background in these regions and lack of shutterability of these peaks made a definite assignment impossible.

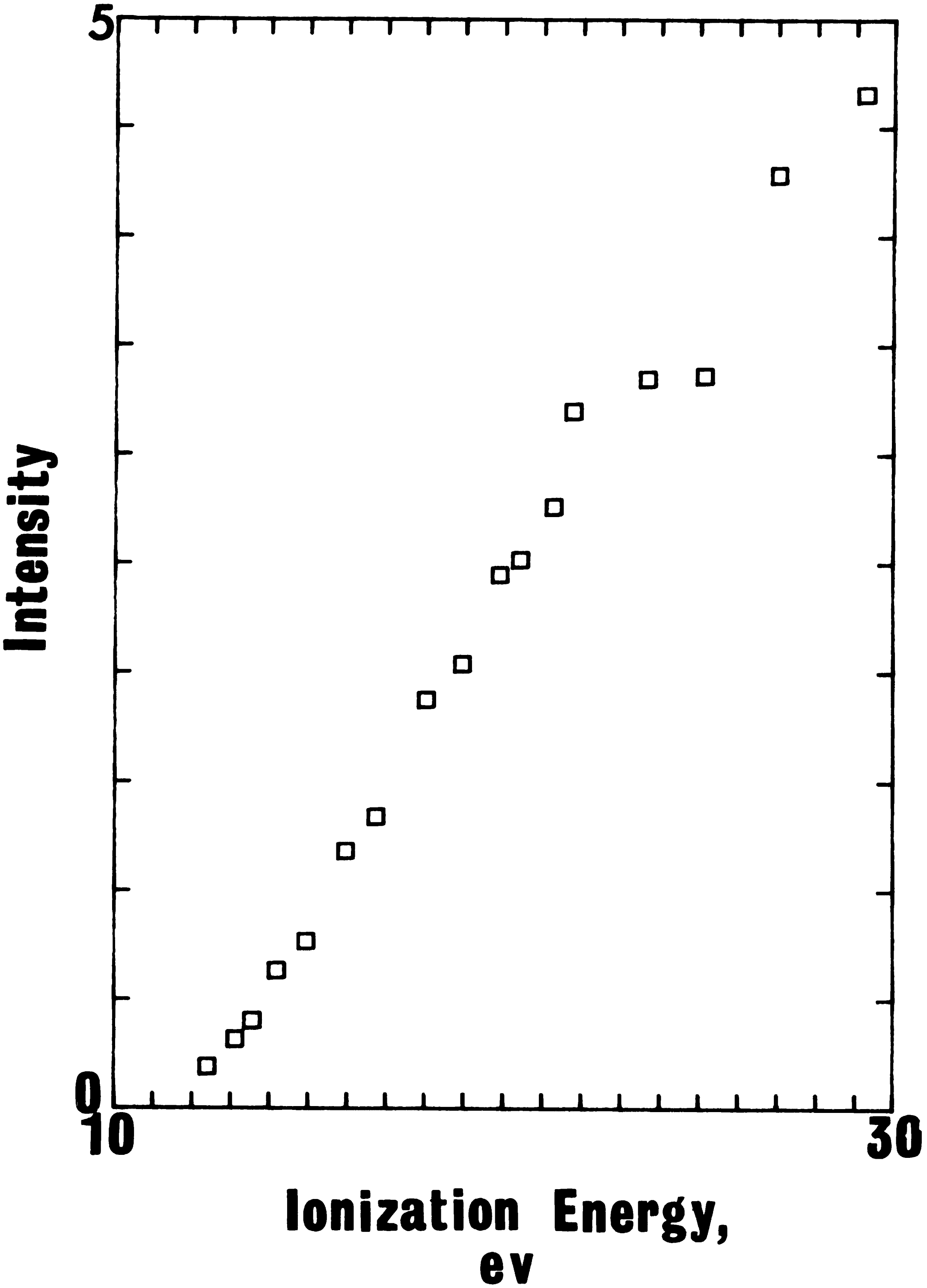

Figure 7. Appearance Potential Curve for EuF^+

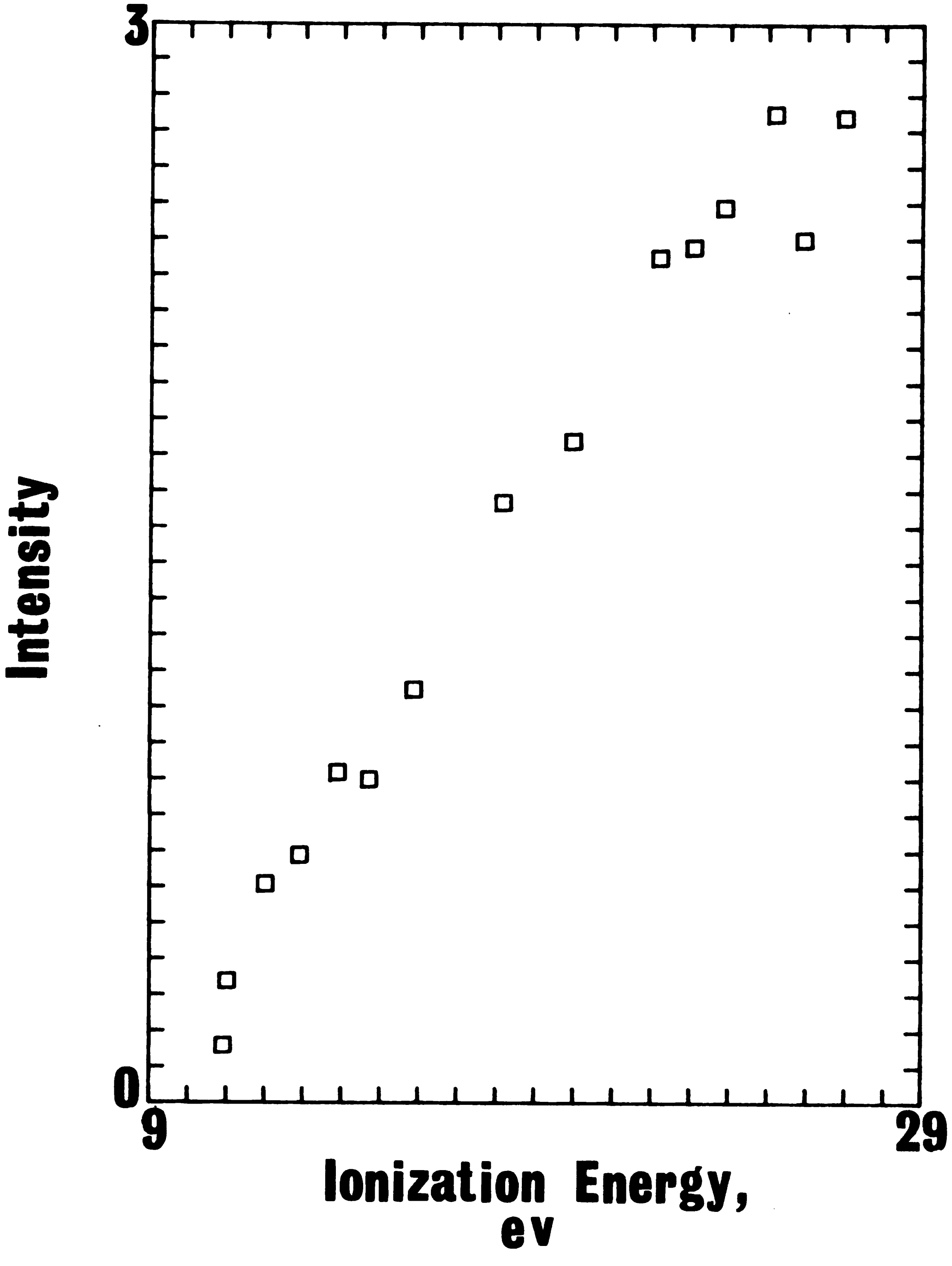

Figure 8. Appearance Potential Curve for EuF_2^+

Table II. Intensity and Appearance Potential Data of the Effusate of EuOF

Shutterable Species		Relative Intensities (at 25 ev)	Appearance Potential
Eu^+	151 153	33	-
EuF^+	170 172	100	12.5 ± 1 ev
EuF_2^+	189 191	24	10.5 ± 2 ev

b. Residue

Residues of a vaporization which had been carried to completion (*i.e.*, Eu_2O_3) showed X-ray diffraction patterns which were characteristic of monoclinic europium sesquioxide plus a cubic pattern. The lines of this cubic pattern were quite faint and only four or five lines could be read. The indexing of these lines yielded a lattice parameter of 5.40 ± 0.01 Å.

Residues which had lost $\geq \sim 90\%$ fluoride as determined by weight loss, contained cubic europium sesquioxide and another cubic phase. This latter cubic phase, when indexed on fcc symmetry exhibited a lattice parameter of 5.50 ± 0.01 Å based on the five lines that could be read.

Any residue which had lost $< \sim 90\%$ of the fluoride showed rhombohedral europium oxidefluoride and cubic sesquioxide. Often the diffraction patterns of these residues had somewhat broad lines rather than the sharp lines characteristic of a well-annealed substance.

The character of the residue seemed more dependent on the percent of fluoride lost, than on temperature of decomposition, although at higher temperatures the sample was more apt to lose all the fluoride because of the increased vapor pressure.

It should also be noted that the color of the residue changed from an off-white through purple to black as the fluoride content was depleted.

c. Attempts to Produce New Phases

The attempts to prepare the two new cubic phases seen in the residue by mixing various amounts of Eu_2O_3 and EuOF proved unsuccessful. In addition, no substantial evidence for solid solution could be obtained even when samples were heated in sealed platinum capsules for times which varied from hours to several days, and were then quenched. Rhombohedral EuOF and cubic sesquioxide were always present. X-Ray diffraction patterns of some samples showed rather broad lines on a random basis.

2. Reaction of Europium Oxidefluoride with Cell Materials

(cf Appendix IV)

a. Molybdenum

Molybdenum Knudsen cells showed no evidence of attack at the end of a vaporization experiment in that the residue fell out readily and all surfaces were shiny and smooth. Weight loss data was not taken with a molybdenum cell, but later vaporization experiments were weighed before and after decomposition. Several of these showed a weight loss of greater than 100% of that expected by analogy to equation (I-1).

The X-ray fluorescence spectrometer was exceedingly sensitive to a small amount of pure powdered molybdenum at its $K\alpha_1$ and $K\alpha_2$ ($2\theta = 12.13$ and 12.21 respectively, graphite monochrometer) emission region. When small amounts of the vaporization residue were scanned in this region, results varied. Residues which had not changed much in color (usually heated below 1400°) showed no evidence of Mo. On the other hand, the deeper the color of the residue, the greater the intensity of the fluorescence at peaks assignable to molybdenum.

One residue which showed B-Eu_2O_3 and the cubic (5.40 ± 0.01 Å) pattern and gave positive results when tested for molybdenum was heated in air. The black residue changed to bright yellow after heating, but evidenced no change in the diffraction pattern. The small weight loss recorded upon heating could not be considered conclusive since the original sample was so small (25 mg).

One sample of effusate which was collected at 1500° from a molybdenum cell also showed the presence of molybdenum but the X-ray fluorescence peak was not very intense.

b. Tungsten

When an 85 mg sample of europium oxidefluoride was completely decomposed in a tungsten cell, a weight loss of $99.4 \pm 0.8\%$ was recorded (*cf.* IV-D-2a). However, the mass of the tungsten cell decreased by 6 mg. The X-ray diffraction pattern of the dark blue residue showed monoclinic Eu_2O_3 and a cubic pattern similar to the one seen when a molybdenum cell was used. The X-ray diffraction lines of the cubic phase in the tungsten cell were more intense than those observed in any of the molybdenum cells, and enough lines were present to confirm that the phase should be indexed on body centered cubic symmetry with a lattice parameter 10.760 ± 0.001 Å.

c. Thoria

Thoria reacted more completely with europium oxidefluoride than either molybdenum or tungsten. After vaporization of EuOF at ∿ 1400° the thoria cup had changed from white to yellow, and brown crystals were growing from the sides and bottom of it. When the residue was shaken loose from the cup, brown crystals could be seen growing out of a yellow solid. No X-ray diffraction lines of either of these phases corresponded with those of Eu_2O_3, EuOF or ThO_2. The brown residue gave a definite hexagonal pattern ($a = 9.590 \pm 0.002$ Å and $c = 7.065 \pm 0.009$ Å). The pattern given by the yellow substance could not be indexed and may represent more than one phase.

The presence of thorium could not be detected readily by X-ray fluorescence. It did not produce sharp intense peaks when a powdered sample was introduced in the X-ray fluorescence spectrometer; the most intense peak was an $L\alpha_1$ emission ($2\theta = 16.4$,graphite monochrometer). When the brown sample was examined for thorium in this 2θ region, no peak could be discerned; examination of the yellow sample produced a small peak.

d. Platinum

When europium oxidefluoride was heated to 1400° in a long platinum tube suspended in the susceptor line, no interaction with the solid was apparent. The residue remained off-white in color and showed

X-ray diffraction lines which correspond to rhombohedral EuOF and cubic Eu_2O_3. The tube was suspended in such a manner that the effusate could collect on the upper walls; however, only a thin gold-colored layer appeared on the lid. This gold-colored layer was scraped off and its X-ray diffraction pattern corresponded to that of two phases, one cubic (a = 5.780 ± 0.005 Å) and one unidentified. X-Ray fluorescence analysis of the residue for Pt gave negative results, but a piece of the upper Pt wall showed intense europium peaks when it was rubbed clean and placed in the spectrometer.

Another test run was made by placing a platinum cup in a molybdenum Knudsen cell gave very different results. No change was found in the platinum cup after the Mo and Pt had been outgassed together at 1500°. The EuOF was then placed in the apparatus and decomposition was effected at 1475°. When the cell was removed from the susceptor line, the residue was dark in color and the now brittle platinum cup had slot like holes in two places. A small piece of the platinum cup which was placed in the X-ray fluorescence spectrometer yielded positive results for molybdenum, but not for europium.

Fluorescence analysis of the effusate and residue evidenced trace amounts of molybdenum, but their X-ray diffraction patterns showed only a cubic pattern (a = 5.790 ± 0.001 Å) and a C-Eu_2O_3-rhombohedral EuOF mixture, respectively.

3. <u>Reaction of Europium Trifluoride with Molybdenum and Platinum</u> (*cf.* Appendix IV)

The condensed effusate of a sample of EuF_3 heated in a molybdenum cell at 1500° appeared as two distinctly colored phases. One which possessed a pinkish beige color gave a fluorescence peak at $2\theta = 12.2$

(graphite monochrometer) characteristic of molybdenum and an X-ray diffraction pattern that could be indexed as cubic (a = 5.791 ± 0.001 Å) plus another set of unidentified lines. The second, a dark brown phase, showed only the lines of the unidentified diffraction pattern described above for the beige phase. This latter phase also gave positive results for molybdenum.

The orange-colored residue showed evidence of melting. No further tests were made on it.

When a platinum tube was used to hold the trifluoride, a clear to white effusate was collected on the upper walls and an orange-gold residue was left in the bottom. Neither effusate nor residue gave any evidence of platinum by fluorescence spectrometry.

X-Ray diffraction analysis of the effusate gave lines which could be matched completely with the reported trifluoride lines, but the intensities of these lines did not correspond to those reported. The residue also showed EuF_3 and a second set of cubic lines (a = 5.78 ± 0.01 Å).

4. Results of Vaporization Experiments

a. Effects of Varying Temperature and Orifice Size

The data collected from initial runs were calculated by use of equation (II-5) on the assumption that EuF_2 was the gaseous species. The pressure of fluorine atoms was then calculated by equation (IV-1)

$$P_F = P_{EuF_2}[M_F/M_{EuF_2}]^{1/2} \qquad \text{(IV-1)}$$

The equilibrium constant, K, was derived and ℓnK was plotted against 1/T. Plots of data collected in the initial runs made by increasing the temperature and then decreasing it failed to yield a straight line. The points fell onto two lines, one line for ascending temperature and another for descending temperatures. A few points from a successive experiment might fall on one of these lines or they might establish a completely new line. It was noticed that in all runs, the last few data points taken seemed to drop below the previous ones of that run regardless of whether temperature was being increased or decreased. Also, when because of a mechanism failure the experiment had to be interupted, the apparatus disassembled and the run started over, the first target collected upon reheating had greater amounts of europium than the last one collected at the same temperature.

The size of the orifice seemed to have no affect on the vaporization results.

b. Results of Constant Temperature Experiments

The temperature could be held within a 5° range over a period of 4 to 5 hours with or without the use of the two color pyrometer and the controller. The controller would hold the temperature steady for a long period, then deviate wildly and settle again to the initial temperature, but the deviation was usually enough to cause the data collected from the target to be rejected.

Figure 9 shows the results of a typical constant temperature experiment. For some of these experiments the total amount of effusate lost was determined by having some target exposed for the entire period of heating. This procedure allowed the average composition of the solid material to be calculated for each target exposed.

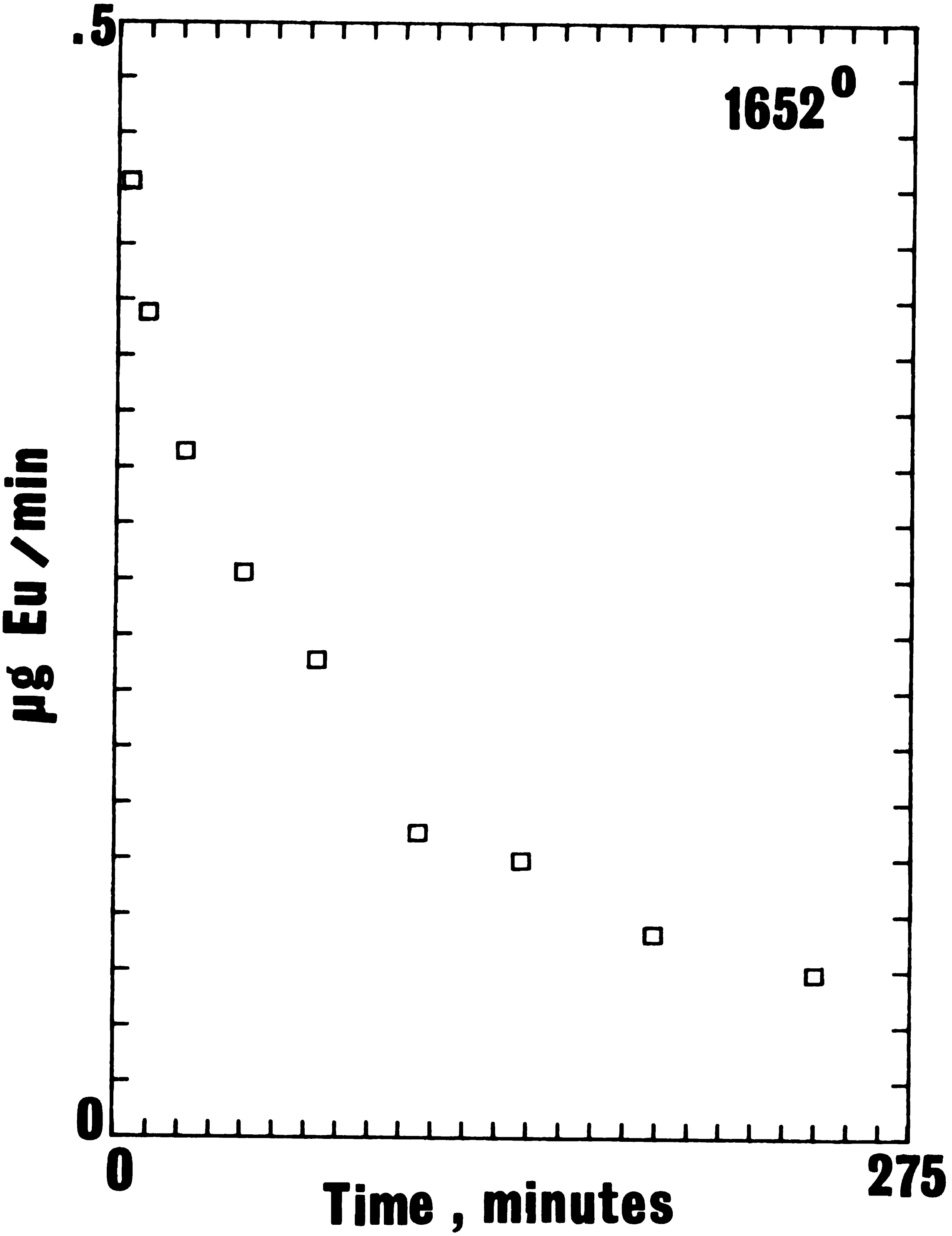

Figure 9. Results of a Constant Temperature Experiment

Appendix II gives the results of these runs calculated on the basis of EuF_2 and F as the gaseous species.

One exception to the drop in vapor pressure with time was found when EuOF was mixed with an excess of monoclinic Eu_2O_3. The pressure dropped off initially but then increased, dropped again and appeared to be increasing on the last target exposed.

E. The Pressure Equation

A pressure equation has not been established for reaction (IV-2)

$$3EuOF_{(s)} \rightarrow Eu_2O_{3(s)} + EuF_{2(g)} + F_{(g)} \qquad \text{(IV-2)}$$

primarily because the pressure does not remain constant with temperature; thus one equation can not represent the entire process. Secondly, in light of the presence of molybdenum in some of the residues, it appears that the pressure measurements may not represent the above reaction. These comments will be discussed later (*cf.* V-B).

F. Thermodynamic Values

In Table III various relevant thermodynamic values are tabulated.

Table III. Reported Thermodynamic Values

Sample	$\Delta H^\circ_{f\ 298}$ in kcal/gfw	fef 1500	Reference
Eu_2O_3 cubic	-386.5	-	41
$EuF_3(s)$	-391.0	-	42
	-411.0	-	43

Table III. (Continued)

	$\Delta H°_{f\ 298}$ in kcal/gfw	fef 1500	Reference
$EuF_2(s)$	-282.0	-	44
	-294.0	-	33
F(g)	18.86	-42.201	45
$F_2(g)$	0	-55.167	45

Estimates of other thermodynamic functions were established in the following manner:

1. Europium Oxidefluoride (solid)

Free energy functions values were obtained for the oxidefluoride by estimating the heat capacity and the $S°_{298}$ value (cf. II-E-3b). The heat capacity data given by Holley *et al.*[40] for the cubic form of europium sesquioxide were used to calculate equation (IV-3).

$$Cp\ (EuOF) = 19._{35} \pm 1._{14} + (1._{72} \pm 1._{02}) \times 10^{-3}\ T - (1._{86} \pm 1._{36}) \times 10^{5}/T^{2} \qquad (IV\text{-}3)$$

A plot of Cp (Eu_2O_3) versus temperature was linear to 1400 K, the highest temperature at which data were reported. Due to its linearity, extrapolation to the temperature range of this study (1500-1850 K) seemed valid.

By use of Latimer's[29] estimates for the entropy contributions of oxygen and fluorine and Westrum's[30] lattice and magnetic contributions for Eu, (cf. II-E-3c), $S°_{298}(EuOF)$ was calculated to be 22.1 ± 1 eu where the error reported is estimated.

The $\Delta H°_{f\ 298}(EuOF)$ was estimated by comparison with Work's[7] reported value for SmOF ($-274._6 \pm 2._5$ kcal/gfw) and reaction (IV-4)

$$C\text{-}M_2O_3 + MF_{3(s)} \rightarrow 3MOF_{(s)} \qquad \text{(IV-4)}$$

The $\Delta H°_r$ for M = Sm was calculated to be 126 ± 14 kcal/gfw.[41,43] This ΔH_r was assumed for the case M = Eu[41,43] to give $\Delta H°_{f\ 298}$ = -224 ± 18 kcal/gfw with the error estimate calculated from $(\sum_i \Delta H_{error_i}{}^2)^{1/2}$.

2. Europium Trifluoride (solid)

Heat capacity data have been measured for many of the lanthanide trifluorides,[47] but unfortunately not for europium. By use of relationship (IV-5)

$$Eu_{(s)} + MF_{3(s)} = EuF_{3(s)} + M_{(s)} \qquad \text{(IV-5)}$$

with the assumption that Δfef for the reaction is zero, the fefs for EuF_3 were interpolated. Free energy functions for M = Pr, Ce, Nd, Gd, and Dy were taken from Hultgren[46] and five values were obtained for fef (EuF_3). These values were then averaged to give the numbers listed in Appendix III.

3. Europium Trifluoride (gas)

A recent spectroscopic study[48] of the structure of $EuF_{3(g)}$ allowed a statistical approach to be used to obtain various thermodynamic functions. Vibrational data were not taken on the gas, but rather on various condensed matricies of the gas and of an inert gas.

Margrave et al.[50] have pointed out that the data obtained with a nitrogen matrix are a more true representation of the real gas than those taken with any other type of matrix gas. Therefore, the reported values[48] of ν_1, ν_2, ν_3 and ν_4 obtained in a N_2 matrix were used for calculating Cp° and $H°_T$-$H°_{298}$ values as discussed in section (II-E-3).

Moments of inertia needed for calculating $S°_T$ require both a value for the bond angle and a bond length. A value of 117° is assigned[48] to the angle F-Eu-F, but no bond length is reported. Other workers[49] have reported bond lengths for La, Y and Nd trifluorides on the assumption of a linear model. By adding the radii[50] of the various +3 metals to the radius of F^- (1.36 Å) a factor (sum of radii - reported bond length) was established to be applied to the sum of Eu^{+3} and F^- radii. This method yielded the bond length of 2.15 Å for EuF_3. Moments of inertia were then calculated to be $I_x = I_y = 2.22 \times 10^{-38}$ and $I_z = 4.24 \times 10^{-38}$. Values obtained subsequently for $S°_T$ are included in Appendix III.

4. Europium Difluoride (solid and gas)

Thermodynamic data have not been published on EuF_2(s). Several estimates do appear in the literature, but these values are quite varied. Since the enthalpy of formation of EuF_2(s) was needed, the enthalpies of formation of the group II fluorides[42] were used as a guide. A value of $\Delta H°_{f\ 298}$ EuF_2(s) (290 $\pm$ 4 kcal/gfw) was chosen by comparison since the enthalpies for the group II fluorides cluster around this number.

The $\Delta H°_{sub\ 298}$ was determined by use of boiling point data,[52] Cp(l → g) (-10 eu) and Cp(s → g) (-6 eu), to be 102 kcal/gfw. From these values ΔH°_f $EuF_2(g)$ is found to be -188 ± 10 kcal/gfw, where the reported error is an estimate.

Other thermodynamic values for EuF_2 gas were obtained by a statistical treatment from the vibrational information reported by Margrave, et al.[50] All parameters needed to calculate Cp°, $H^\circ_T-H^\circ_{298}$ and S°_T were taken directly from Margrave's paper. These values are reported in Appendix III.

G. Thermodynamic Results

1. Results of Various Estimations

In the course of interpreting the pressure data taken in this study, the possibility of several reactions was encountered. In an effort to decide which was thermodynamically most possible, the enthalpies of various reactions were investigated. Most crucial to interpretation were reaction (IV-6) to (IV-8).

$$EuF_{3(g)} \rightarrow EuF_{2(g)} + F_{(g)} \qquad \text{(IV-6)}$$

$$EuF_{3(s)} \rightarrow EuF_{2(g)} + F_{(g)} \qquad \text{(IV-7)}$$

$$EuF_{2(g)} + F_{2(g)} \rightarrow EuF_{3(g)} + F_{(g)} \qquad \text{(IV-8)}$$

For equation (IV-6) combination of $\Delta H^\circ_{f\ 298}(EuF_{3(g)})$ = -310 kcal[43] and $\Delta H^\circ_{f\ 298}(EuF_{2(g)})$ values of a) -160 kcal/gfw[43] or b) -188 kcal/gfw (cf. IV-F-4) yield ΔH°_{298} values of 141 ± 14 kcal/gfw or 169 ± 14 kcal/gfw, respectively. By combining these data with the free energy functions established in the statistical treatment (Appendix III) an equilibrium constant of 7.97×10^{-8} was calculated for reaction (IV-6) at the highest temperature studied (1838 K). (Note that ΔH°_f EuF_2 is taken as -188 kcal/gfw in this as well as in subsequent calculations.)

The $\Delta H°_{298}$ for equation (IV-7) is found to be 242 ± 14 kcal/gfw. From this value and the free energy functions a $\Delta G°_{1838}$ of 104 ± 20 kcal/gfw is obtained.

Equation (IV-8) has a pressure independent equilibrium constant and also contains the well established equilibrium constant for reaction (IV-9).

$$F_2 \rightarrow 2F \qquad \text{(IV-9)}$$

The value of K_{1600} for reaction (IV-8) was found to be 7.47×10^{10} from the enthalpies and fefs discussed above.

2. Results of Thermodynamic Reduction of the Data

Since an equation could not be established definitely for the reaction taking place in this study the data could not be reduced. When the reaction is established methods discussed in II-E-2 may be applied for obtaining $\Delta H°_{298}$ values.

V. Discussion

A. Preparative Work

It is most interesting that a 1:1 mixture of monoclinic Eu_2O_3 and EuF_3 produce phase pure EuOF while the same mixture of cubic Eu_2O_3 and EuF_3 always showed excess Eu_2O_3 in the final product. The full significance of this behavior is not understood, but could be due to the formation of solid solution between the cubic oxide and EuF_3. This possibility will be discussed later.

It should also be pointed out that the preparations which resulted in excess sesquioxide were used for the bulk of the vaporization experiments on the assumption that since Eu_2O_3 is one of the equilibrium products, its presence would not interfere and, if anything, would hasten attainment of equilibrium. Vapor pressure measurements bore out the validity of this assumption, since both the pure EuOF sample and those which contained excess C-form oxide gave consistent results.

B. Characterization of Mode

Mass spectrometry results seem rather conclusive that EuF_2 is one of the vapor species. Appearance potentials of the ionic species generated by electron bombardment from EuF_3[53] are reported to be 13.5 ± 0.7 ev, EuF_2^+; 19.5 ± 0.7 ev, EuF^+; and 27.0 ± 0.7 ev Eu^+. Although the appearance potential of EuF_2^+ from EuF_3 found in this study (10.5 ev) is fairly close to the reported value that for EuF^+

is markedly different. No break in intensity could be found around 19 ev as the ionization energy was decreased, an indication that EuF_3 was not providing any of the EuF^+ species present. Other evidence which supports the fact that EuF_2 is the only neutral species is the work done on the Group II fluorides.[54-56] The appearance potentials of these parent ions and the parent minus one fluorine ion are very similar in value (∿ 12-13 ev). Also, in the study of MgF_2,[56] the only species for which the MF_2^+ intensity is adequate for interpretation, the intensity ratio of the ionic species, Mg^+, MgF^+, MgF_2^+, is very similar to that seen in this study.

The X-ray diffraction data of the effusate are not so conclusive as the mass spectrometry. The cubic pattern which appears regardless of temperature or cell material does not coincide with the lattice parameter (a = 5.840 Å) reported for $EuF_{2.00}$.[57] Catalano and Bedford have completed a moderately extensive study on the phases which exist between EuF_2 and EuF_3. They report a composition region from $EuF_{2.29}$-$EuF_{2.44}$ which has an unsolved structure, but its strongest lines can be indexed on an fcc cell with a = 5.78 Å. The color of the phases which possess this composition vary from dark brown to brown. Both the lattice parameter and color correspond to the effusate collected from EuOF. It is also noteworthy that this same range of stoichiometry was duplicated time after time even though the temperature of the collection surface was not controlled and the temperature of the reaction was varied. The most reasonable explanation for this consistency is that EuF_2 and F are evolved and some interaction occurs as the two hit the collection surface. The composition range

$EuF_{2.29}$-$EuF_{2.44}$ may be a particularly stable region and therefore easily reproduced, and beyond the composition $EuF_{2.44}$ only EuF_3 is an allowed second phase.

A mixture of $EuF_3(g)$ and $EuF_2(g)$ seems to be ruled out on the basis of mass spectrometer results. If EuF_3 were one of the species, it should be more abundant at lower temperatures, yet no peak could be found even at 1290°. However, the possibility of an $EuF_2(g)$ and $MoF_x(g)$ mixture can not be ruled out. The effusate does evidence molybdenum when examined on the X-ray fluorescence spectrometer. Mass spectrometry was not useful in supporting this conclusion since the unshutterable background in the region Mo^+ to MoF_4^+ is very intense, and molybdenum has a large number of isotopes.

The analysis of residue, on the other hand, proved to be more straightforward. The oxidefluoride definitely decomposes to the cubic form of the sesquioxide with no intermediate phases. The two other cubic phases will be discussed in the following sections.

C. Interpretation of Pressure Measurements

The exponential type drop in pressure with time at constant temperature may be explained by either a diffusion controlled process (cf. II-A-2a) or a reaction which has more than one degree of freedom (cf. II-D-3). A diffusion problem alone does not seem to be the case since cooling a sample and reheating it to the same temperature gives a pressure increase rather than that pressure recorded before the cooling-reheating cycle occurred. Diffusion is caused by a change in surface composition and cooling and reheating should not change this composition. The pressure should be the same.

All evidence points toward solid solution formation between EuOF and Eu_2O_3, a case in which F = 2 (C = 2 and P = 2). As the solution is formed the vapor pressure is lowered, and as the sample under study becomes depleted in fluoride, the pressure falls off even more. The tendency of pressure to increase on cooling and subsequent reheating indicates that the solid solution is temperature dependent. Apparently the solution is not formed completely as the sample is heated, so the higher vapor pressure of the pure oxidefluoride must be present initially. Another indication of the temperature dependence of this solution is the fact that the cubic form of the sesquioxide and the rhombohedral form of EuOF are present by the time the residue of a vaporization has reached room temperature. Only two of the many samples that were studied gave any X-ray diffraction evidence of the solid solution, and those were the ones where the rhombohedral EuOF had not completely grown in, but an fcc pattern ($a = 5.50 \pm 0.01$ Å) was observed instead. Since Shinn[4] reports that cubic EuOF has a lattice parameter of 5.535 Å, this new phase is probably the solid solution. The a = 5.50 Å parameter is intermediate between that of cubic EuOF and that of Eu_2O_3 indexed on fcc (a = 5.433 Å) rather than on bcc (a = 10.866 Å)[39] symmetry.

It is very reasonable that a solution would form between C-Eu_2O_3 and EuOF at high temperatures. Above 600° EuOF has a fluorite structure[4] and Eu_2O_3 itself has a structure which is based on fluorite with only anion vacancies. A number of examples of fluorite structures which form solid solutions have been reported in the literature;[3,6,59,60] many systems closely related to that under study have been proven to have regions of solid solution. The most pertinent is the EuF_3-EuOF system studied by Catalano and Bedford.[3] They point out the availability of interstitial holes in the EuOF fluorite lattice, and they reason that a pair of fluoride ions enters these vacancies as the solution is formed. Initially as only a slight excess of F^- is introduced the cubic structure is distorted tetrahedrally and then as the fluoride concentration is increased a solid solution which is stable at room temperature forms.

Other examples of fluorite type solid solutions are the EuF_2-EuF_3[57] system, the ThO_2-ThOF[59] system and the ThO_2-Eu_2O_3[60] system in addition to other MF_3-MOF[6] systems. All of these observations substantiate the ability of Eu_2O_3 and the fluorite type EuOF to form solutions.

Some comment on the stability of the solution formed between Eu_2O_3 and EuOF can also be made from the results obtained in this study. It is definitely temperature dependent. Apparently the stability of the rhombohedral form of EuOF at room temperature is the cause of this behavior. If one pictures the formation of solution to result from the ability of the fluoride ions to migrate through the Eu_2O_3 lattice at high temperatures and situate themselves in the vacancies of the bcc structure as temperature is lowered, cubic EuOF could result in the midst of Eu_2O_3. Brauer and Roether[5] report that $MO_{1.0}F_{1.0}$ (M = La, Nd, Sm and Gd) in the cubic form cannot be quenched. Thus, since the solution may contain only $EuO_{1.0}F_{1.0}$ surrounded by Eu_2O_3, it may not be quenchable.

D. Effect of Cell Material on the Reaction (cf Appendix IV)

1. Molybdenum

Molybdenum was originally chosen for use as cell material since the study of SmOF had been completed in molybdenum with no apparent interaction. No weight loss data were taken initially since the first few X-ray diffraction patterns showed no new phases in either the residue or effusate. The fact that EuF_2 appeared as a gaseous species was thought to indicate that EuF_2 was the more stable gaseous species and not that cell material was interferring. It was not until one of the later vaporization experiments that the fcc phase (a = 5.40 ± 0.01 Å) was seen. This cell is even smaller than those of EuOF or the sesquioxide and it was hard to explain why a solution of these two would cause a decrease in cell size. Molybdenum, which is a smaller atom than europium, could be replacing some of the europium in the cubic lattice and thus shrinking the cell size.

2. Tungsten

The reaction between EuOF and tungsten seems to confirm the idea of interaction cited above. With tungsten, this new cubic phase was more intense in the X-ray diffraction pattern, indicative that tungsten was more reactive to EuOF than molybdenum. Enough lines appeared in the pattern to define the cell as body centered cubic, and therefore to double the cell parameter to a = 10.760 ± 0.001 Å. This observation seemed to confirm that the bcc Eu_2O_3 was being affected as was suspected in the case of molybdenum. A literature search produced no reports of a cubic europium tungstate or molybdate, however.

The mechanism of the reaction of EuOF with W or Mo is not yet understood, but it is apparent that molybdenum appears in both the solid and effusate. One explanation of this phenomenon is that gaseous EuF_3 escapes from the solid solution and interacts with the cell walls forming some molybdenum fluoride and europium difluoride.

The molybdenum fluoride vapor can then either escape through the orifice or react with the solid solution, displacing more europium from it.

The results of a test in which $EuF_3(s)$ was evaporated in a molybdenum cell gives some support to this premise; a substantial amount of molybdenum was found in the effusate along with a new phase, the X-ray diffraction pattern of which does not match any known europium-fluorine phases. This observation is confusing since the vaporization study of EuF_3 was carried out in molybdenum or graphite.[53] A more recent article[50] has reported that reaction (V-1) occurs in graphite cells, and my research gives similar results with molybdenum.

$$EuF_{3(s)} \rightarrow EuF_{2(g)} + 1/2\ F_{2(g)} \qquad \text{(V-1)}$$

Catalano and Bedford[3,57] report reaction with molybdenum in both the case of EuF_3 and fluorine rich samples of $EuO_{1-x}F_{1+2x}$ and also remark that the trifluoride is an unstable, ill-defined substance above 1400°. However, they do not elaborate in this later report as to what is happening to the EuF_3.

When molybdenum and tungsten proved to be the improper choice of cell material, platinum and thoria were tried.

3. Thoria

The small brown crystals which formed from the reaction of EuOF with thoria yielded a hexagonal diffraction pattern. Attempts to find one crystal suitable for a single crystal structural analysis proved difficult. On the basis of the X-ray diffraction pattern and a few single crystal layer pictures that were obtained, the structure appears to belong to the apatite family. This structure was realized when it was noted that the same pattern (with lattice parameter shifts) appeared in the diffraction patterns of the green powder scraped from the walls of a quartz tube in which EuOF had been heated, and the pink powder from a quantz and a thoria cup used in a study of SmOBr by D. E. Work. A literature search produced the apatite structures $Sm_4(SiO_4)_3$,[61] a = 9.497, c = 6.949 Å, $Ce_{4.67}(SiO_4)_3O$,[62] a = 9.659, c = 7.121 and $La_5(SiO_4)_3O_{1.5}$,[63] a = 9.72, c = 7.20, all of whose intensity data matched those seen in the films of the EuOF and SmOBr reactions.

By using the program ANIFAC the observed intensities and interplanar spacings could be recreated for both the europium and samarium silicates for the empirical formula $Ln_{4.67}(SiO_4)_3O$ with the atomic position reported for $Ca_5(PO_4)_3F$[64] (<u>cf.</u> Appendix V). The apatite structure found in the thoria cup proved more difficult to regenerate. The intensities of the Eu-Th compound are very similar to those observed in the Eu-Si structure, but use of the formula $Eu_{4.67}(ThO_4)_3O$ in the program ANIFAC gives intensities which do not match the observed pattern at all. Further investigation revealed that some apatite compounds have the general formula $A_3B_2(CO_4)_3X$.[64] The compound $Eu_3Th_2(EuO_4)_3O$ fits this general formula and its generated intensity data is much closer to that observed in the X-ray diffraction pattern. The exact positioning of the europium and thorium atoms could bring the intensities into the proper perspective, but such positioning can not be undertaken without the availability of single crystals. If such crystals can be obtained the confirmation of the proposed structure would be of value due to the unusual tetrahedral arrangement around the europium.

4. Platinum

Platinum did not prove to be a satisfactory cell material either. Not only does it react with molybdenum so that a Knudsen cell would have to be machined completely from it, but it also showed evidence of gas phase attack since the upper walls contained europium.

It is interesting that europium was abstracted into the Pt. Catalano and Bedford[65] report that such a reaction occurs only with the difluoride. This observation would indicate that EuF_2 was the gaseous species. Indeed, this thought is consistent with the results obtained in molybdenum, but EuF_3 is not reduced by platinum according to further work by Catalano and Bedford.[57] My own results of the sublimation of EuF_3 in Pt do not clarify this point (cf. Appendix 4). The effusate appears to remain untouched (EuF_3) while the residue has been reduced ($EuF_{2.5}$-$EuF_{2.9}$)

E. Unanswered Questions and Their Possible Resolution

1. What Is the Reaction with Molybdenum?

As section V-D-2 infers, it is believed that either condensed EuOF or gaseous EuF_3 is reacting with the molybdenum, thus mobilizing the molybdenum so that it ends up in both the effusate and the residue. Such reaction requires the formation of a molybdenum fluoride or some mixed Eu-Mo fluoride. If there were thermodynamic data on either of the types of fluorides, the possibility of several reactions could be investigated. Unfortunately, few molybdenum fluorides have been studied thermodynamically. Since the question can not be answered theoretically perhaps other tests may shed some light on the problem. By suspending a strip of Mo over EuOF in the same manner as described by Catalano and Bedford[65] in their study of Eu-Pt alloys, one could determine if the reaction was strictly a gas phase or not. Further tests with EuF_3 and Mo might also be helpful.

It is obvious that the solution to this question is important since it would allow interpretation and data reduction of the pressure measurements made in this study.

2. What Is The Mode of Vaporization of EuOF?

The only way to answer this question is to find some refractory substance that will not react with EuOF at temperatures up to 1600° and possibly higher. Since the cell material interfered, the temperature range for a vaporization study could be considerably higher than that observed in this study. Suggestions for cell material are limited to a fluoride passified nickel for temperatures below 1400°, and some type of platinum alloy. A platinum-rhodium or platinum-iridium alloy would give the needed temperature range and possibly passify the platinum so that it would not interact.

3. Does $EuF_{3(s)} \rightarrow EuF_{3(g)}$? How Does This Reaction Affect the Vaporization of EuOF?

From the existing thermodynamic estimates (*cf.* IV-E G-1) EuF_3 is the more stable gaseous species at the temperatures of this study. It would, therefore, be expected to be one of the equilibrium products of the decomposition of EuOF. There is definite reason to question the $\Delta H_s(EuF_3)$ value reported by Margrave[53] since more recent works report the reduction of EuF_3 (*cf.* V-E-1) by Mo and graphite, the materials used in the sublimation study. If indeed this value of ΔH°_s is in error, the estimate of ΔH_f $EuF_3(g)$ would be altered possibly to the extent where $EuF_2(g)$ would be the more stable gaseous species at high temperatures. Catalano and Bedford[57] report a pressure build up for the compositions $EuF_{2.5}$-$EuF_{2.99}$ in sealed capsules at 1600°, but no such build up for the lower fluorides. Their observation indicates that $EuF_{2(s)}$ is more stable with respect to vaporization than $EuF_{3(s)}$ at 1600°, although it still must be questioned whether the cell interfered (a Pt-10% Rh alloy was used). The stability of EuF_2 over EuF_3 would refer to a $\Delta G°_T$ of sublimation which would be more negative for EuF_2. If $EuF_{3(s)} \rightarrow EuF_{3(g)}$ at this temperature and $EuF_{2(s)} \rightarrow EuF_{2(g)}$ then the entropies of the two reactions must be reasonably similar leaving the enthalpies as the thermal quantities which differ. On the other hand, if $EuF_{3(s)} \rightarrow EuF_{2(g)} + F_{(g)}$ then the additional entropy gain over $EuF_{2(s)} \rightarrow EuF_{2(g)}$ could be enough to cause the reaction to go at lower temperatures than $EuF_{2(s)} \rightarrow EuF_{2(g)}$. Further study on both EuF_2 and EuF_3 are required before any of these suppositions can be justified.

4. Why the Difference Between SmOF and EuOF?

There are many other inferences which can be made from this study which unfortunately lack much substantiation. One such inference is that the enthalpy of formation of EuOF is more positive than that of SmOF. Measureable vapor pressures were recorded for EuOF at temperatures much lower than those for SmOF.[7] However, the interference of molybdenum may have been enough to increase the activity of Eu to give the greater pressure at lower temperatures, since SmOF showed no evidence of reaction with molybdenum. The estimated enthalpy of formation of EuOF (<u>cf.</u> IV-F-1) is substantially lower than that of SmOF since it is based on the known difference between the enthalpies of formation of Eu_2O_3 and Sm_2O_3.

Another basic question which can not be answered with existing data is why Sm and Eu compounds behave so differently. The unusual behavior of europium compounds in molybdenum has been noted by another worker[66] when he studied the vaporization of EuOBr and SmOBr in molybdenum. The europium oxidebromide reacted with the Mo to the extent that europium molybdate lines were identified in the X-ray diffraction pattern. The SmOBr gave no evidence of attack with weight loss data equaling 100% of theoretical.

5. Further Comments

Continuation of the study of solid solution formation between EuOF and the sesquioxide would be of value. It is possible that at high temperatures (in the range of 1200°-1600°) EuOF may not be a compound but rather a 1:1 solution of EuF_3 dissolved in Eu_2O_3. From vapor pressure measurements made on EuOF with no cell interference the activity of the species in solution may be calculated and further data reduction allowed (cf. II-E-1). If EuF_3 is the species in solution, the activity data should extrapolate to the pressure of $EuF_3(g)$ over pure $EuF_3(s)$. Further information about the activity of the trifluoride could be gained also by studying the vaporization behavior of the fluoride rich side of EuOF.

It is unfortunate that the interpretation of my study depends so heavily on estimates and the observations of only two other groups, that of Catalano and Bedford[3,57,64] and that of Margrave et al.[48,50,53] The contradictory results can not be solved unless the thermodynamics of EuF_2 and EuF_3 are investigated more deeply in cognizance of the various cell materials which interfere.

BIBLIOGRAPHY

BIBLIOGRAPHY

1. V. W. Klemm and H. A. Klein, *Z. anorg. allg. Chem.*, **248**, 167 (1941).
2. W. H. Zachariasen, *Acta Cryst.*, **4**, 231 (1951).
3. R. G. Bedford and E. Catalano, *J. Solid State Chem.*, **2**, 585 (1970).
4. D. B. Shinn, Ph.D. Thesis, Michigan State University, East Lansing, MI (1968).
5. G. Brauer and U. Roether, Proceedings of the 7th R. E. Research Conf., Volume 1, Colorado, 253 (1968).
6. D. J. M. Bevan, R. S. Cameron, A. W. Mann, G. Brauer and U. Roether, *Inorg. Nucl. Chem. Letters*, **4**, 241 (1968).
7. D. Work and H. A. Eick, *J. Phys. Chem.*, **74**, 3130 (1970).
8. J. L. Margrave, "Physicochemical Measurements at High Temperatures", J. Bockris, J. L. White, and J. D. MacKenzie, eds., Butterworths Scientific Publications, London (1959) p 225.
9. K. D. Carlson, "The Characterization of High Temperature Vapors", J. L. Margrave, ed., Wiley, New York, N.Y. (1967) p 115.
10. P. Clausing, *Physica*, **9**, 65 (1929).
11. J. W. Ward, AEC Report, LA-3509, Los Alamos, N.M. (1966).
12. R. D. Freeman and J. G. Edwards, "The Characterization of High Temperature Vapors", J. L. Margrave, ed., Wiley, New York, N.Y. (1967) p 508.
13. R. A. Kent, Ph.D. Thesis, Michigan State University, East Lansing, MI (1963).
14. R. J. Ackermann, R. J. Thorn, and G. H. Winslow, "The Characterization of High Temperature Vapors", J. L. Margrave, ed., Wiley, New York, N.Y. (1967) p 427.
15. G. M. Rosenblatt, P. Lee, and M. B. Dowell, *J. Chem. Phys.*, **45**, 3454 (1966).
16. R. Grimley, "The Characterization of High Temperature Vapors", J. L. Margrave, ed., Wiley, New York, N.Y. (1967) p 195.

17. G. H. Stout and L. H. Jensen, "X-Ray Structure Determination - A Practical Guide", MacMillian, New York, N.Y. (1968).

18. W. Parrish, "Advances in X-Ray Diffraction", Centurex Publishing Co., Eindhover (1962).

19. R. L. Seiver, AEC Report COO-716-067 (1970).

20. J. L. Margrave, "Physicochemical Measurements at High Temperatures", J. Bockris, J. L. White, and J. D. MacKenzie, eds., Butterworths Scientific Publications, London (1959) p 6.

21. A. Findlay, "The Phase Rule and Its Applications", A. N. Campbell, N. O. Smith, eds., Dover Publications (1951).

22. J. Haschke, Ph.D. Thesis, Michigan State University, East Lansing, MI (1969).

23. G. N. Lewis and M. Randall, "Thermodynamics", Revised by K. S. Pitzer and L. Brewer, McGraw Hill Book Co., Inc., New York, N.Y. (1961).

24. K. K. Kelley and E. G. King, Bureau of Mines Bulletin 592, U. S. Government Printing Office, Washington, D.C. (1961).

25. L. L. Ames, P. N. Walsh, and D. White, *J. Phys. Chem.*, **71**, 2707 (1967).

26. S. Smoes, P. Coppens, C. Bergman, and J. Drowart, *Trans. Farad. Soc.*, **65**, 682 (1969).

27. E. A. Hoelwyn-Hughes, "Physical Chemistry", 2nd ed, Pergamon Press, New York, N.Y. (1961).

28. K. K. Kelly, Bureau of Mines Bulletin 584, U. S. Government Printing Office, Washington, D.C. (1960).

29. W. M. Latimer, "Oxidation Potentials", 2nd ed., Prentice Hall, Englewood Cliffs, N.J. (1952), Appendix III.

30. E. F. Westrum, Jr., "Advances in Chemistry Series", No. 71, American Chemical Society, Washington, D.C. (1967).

31. J. J. Stezowski, Ph.D. Thesis, Michigan State University, East Lansing, MI (1968).

32. P. A. Pilato, Ph.D. Thesis, Michigan State University, East Lansing, MI (1968).

33. D. Brown, "Halides of the Lanthanides and Actinides", Wiley, New York, N.Y. 1968.

34. R. H. Powell and O. Menis, *Anal. Chem.*, **30**, 1546 (1958).

35. A. C. Larson, R. B. Roof, D. T. Cromer, U. S. Atomic Energy Commission Report LR 3335, Los Alamos, N.M. (1965).

36. S. Megregian, *Anal. Chem.*, **26**, 1161 (1954).

37. R. W. G. Wyckoff, "Crystal Structures", Vol. II, Interscience Publishers, New York, N.Y. (1964).

38. N. C. Baenziger, J. R. Holden, G. E. Knudsen, and A. I. Popov, *J. Amer. Chem. Soc.*, **76**, 4734 (1954).

39. S. Geller, P. Romo, and J. P. Remeika, *Zeit. fur Kristallographie*, **124**, 1361 (1967).

40. D. T. Cromer, *J. Phys. Chem.*, **61**, 753 (1957).

41. C. E. Holley, Jr., E. J. Huber, Jr., F. B. Baker, "Progress in the Science and Technology of the Rare Earths", L. Eyring ed. Vol. 3, 343, Pergamon Press, New York, N.Y. (1968).

42. L. Brewer, G. R. Somayajulu, and E. Brackett, *Chem. Rev.*, **63**, 111 (1963).

43. K. F. Zmbov and J. L. Margrave, *J. Inorg. Nucl. Chem.*, **29**, 59 (1967).

44. C. E. Wicks and F. E. Block, Bureau of Mines Bulletin 605, U. S. Government Printing Office, Washington, D.C. (1963).

45. "Janaf Thermochemical Tables", D. R. Stull, ed., Dow Chemical Co., Midland, MI (1965).

46. R. Hultgren, R. L. Orr, P. D. Anderson and K. K. Kelley, "Supplement of Selected Values of Thermodynamic Properties of Metals and Alloys", private communication, R. Hultgren.

47. J. V. Charlee, A. K. Chaudhuri, and J. L. Margrave, *High Temp. Sci.*, **2**, 1 (1970).

48. R. H. Hauge, J. W. Hastie and J. L. Margrave, *J. Less Common Metals*, **23**, 359 (1971).

49. P. A. Akishin, N. G. Rambidi and V. P. Spiridonov, "The Characteriation of High Temperature Vapors, J. L. Margrave, ed., Wiley, New York, N.Y. (1967).

50. J. W. Hastie, R. H. Hauge and J. L. Margrave, *High Temp. Sci.*, **3**, 56 (1971).

51. F. A. Cotton and G. W. Wilkinson, "Advanced Inorganic Chemistry", 2nd ed., Interscience Publishers, Wiley, New York, N.Y. (1966).

52. L. Brewer, "The Chemistry and Metallurgy of Miscellaneous Materials", L. L. Quill, ed., McGraw Hill, New York, N.Y. (1950) paper 8.

53. K. F. Zmbov and J. L. Margrave, "Advances in Chemistry Series", #72, American Chemical Society, Washington, D.C. (1968).

54. D. L. Hildenbrand, *J. Chem. Phys.*, **48**, 3657 (1968).

55. J. W. Green, G. D. Blue, T. C. Ehlert, and J. L. Margrave, *J. Phys. Chem.*, **41**, 2245 (1964).

56. J. Berkowitz and J. R. Marquart, *J. Chem. Phys.*, **37**, 1853 (1962).

57. E. Catalano, R. G. Bedford, V. G. Silveira, and H. H. Wickman, *J. Phys. Chem.*, **30**, 1613 (1969).

58. A. F. Wells, "Structural Inorganic Chemistry", 3rd ed., Clarendon Press, Oxford (1962).

59. J. Lucas and J. P. Rannou, *C. R. Acad. Sci. Paris, Ser C*, **266**, 1056 (1968).

60. Von K. A. Gingerick and G. Brauer, *Zeit. anorg. allg. Chem* , **324**, 48 (1963).

61. G. J. McCarthy, W. B. White, and R. Roy, *J. Inorg. Nucl. Chem.*, **29**, 253 (1967).

62. J. Felsche, *Naturwissenschaften*, **56**, 325 (1969).

63. J. Felsche, *Ibid.*, **56**, 212 (1969).

64. R. W. G. Wyckoff, "Crystal Structures", Vol. III, Interscience Publishers, New York, N.Y. (1965).

65. R. G. Bedford and E. Catalano, Proceedings 8th R. E. Research Conf., Reno, Nevada (1970).

66. D. E. Work, Michigan State University, private communication (1971).

APPENDICES

Appendix I

X-Ray Diffraction Analysis

EuF_3 orthorhombic $\lambda = 1.54050$ Å

CALCULATED		OBSERVED	
Intensity	$\sin^2\theta$	$\sin^2\theta$	$hk\ell$
19.9	.0427	.04237	011
56.0	.0442	.04389	101
59.4	.0482	.04785	020
100.0	.0563	.05592	111
76.8	.0662	.06585	210
3.6	.0848	.08454	201
34.2	.0924	.09225	121
2.6	.0969		211
1.6	.1023		220
16.1	.1228	.12257	002
31.8	.1330	.13285	221
3.9	.1363		102
41.6	.1484	.14825	112
46.2	.1525	.15245	301
67.0	.1526	.15245	131
62.4	.1625	.16253	230
37.6	.1646	.16462	311
28.3	.1710	.17112	022
31.6	.1845	.18447	122
42.2	.1890	.18901	212
25.1	.1927		
35.3	.2006	.20076	321
19.1	.2165	.21700	400
18.8	.2369	.23687	141
3.7	.2446	.24490	302
13.0	.2447		132
15.2	.2566		312
11.5	.2592		411
24.0	.2609		331
17.9	.2646	.26481	420
7.6	.2775		241
23.4	.2853		232
17.6	.2884		013
7.9	.2927		322
6.2	.3019		113
12.9	.3155		042
2.5	.3249		430
9.4	.3290		142

EuF_3 orthorhombic (Continued)

CALCULATED		OBSERVED	
Intensity	$\sin^2\theta$	$\sin^2\theta$	hkℓ
15.4	.3304	.33043	203
4.5	.3318		051
6.4	.3380		123
9.4	.3393		402
25.6	.3451	.34559	341
14.0	.3453		151
2.8	.3530		332
12.1	.3552		250
4.0	.3556		431
5.8	.3689		501
36.5	.3786	.37862	223

EuOF rhombohedral $\lambda = 1.54050$ Cu K_1

a = 6.827
α = 33.05

CALCULATED			OBSERVED
hkℓ	$\sin^2\theta$	Relative Intensity	$\sin^2\theta$
111	.0143	6.6	.0139
222	.0571	29.4	.0568
110	.0588	100.0	.0586
211	.0778	35.8	.0776
221	.0921	4.4	
333	.1284	2.2	.1281
322	.1301	4.6	.1299
332	.1539	11.4	.1537
$10\bar{1}$	.1573	12.7	.1575
433	.2110	2.7	.2112
321	.2144	7.1	.2143
200	.2161	4.1	.2160
220	.2352	2.6	.2351
443	.2443	1.5	
432	.2858	2.2	
422	.3113	3.4	
544	.3204	1.4	
442	.3683	1.3	
$21\bar{1}$	.3735	3.7	.3732
543	.3856	1.1	
310	.3925	2.0	.3913

Eu_2O_3 cubic λ = 1.54050 a = 10.866 Å

CALCULATED			OBSERVED
hkℓ	$\sin^2\theta$	Intensity	$\sin^2\theta$
112	.0301	5.6	.0300
222	.0602	100.0	.0602
123	.0702	1.4	.0701
004	.0804	33.1	.0802
114	.0904	4.4	.0903
042	.1004	0.7	
233	.1104	5.1	.1103
134	.1305	4.2	.1304
125	.1506	0.8	.1506
044	.1607	12.2	.1606
334	.1705	0.5	.1705
116	.1908	0.6	.1906
145	.2108	0.9	.2107
226	.2208	9.6	.2207
163	.2309	1.8	.2309
444	.2408	2.4	.2406
345	.2508	0.8	.2508
336	.2709	0.5	.2709
127	.2711	0.5	
246	.2810	0.5	
237	.3112	0.9	
008	.3216	1.7	.3200
455	.3311	0.5	
147	.3313	0.5	.3310
118	.3315	0.6	
356	.3512	0.7	
266	.3814	2.9	

Appendix II

Vapor Pressure Measurements

III-B G.F. = 206.273 $a_o = .01012\ cm^2$

Time	μgEu	T°K	P_{EuF_2}	P_F	Composition
30.00 min	11.172	1598	$1.0348x10^{-5}$	$3.2727x10^{-6}$	$EuO_{1.065}F_{.87}$
30.00	6.120	1598	$5.6687x10^{-6}$	$1.7928x10^{-6}$	$EuO_{1.10}F_{.80}$
29.92	5.402	1603	$5.0236x10^{-6}$	$1.5887x10^{-6}$	$EuO_{1.12}F_{.77}$
30.20	4.999	1598	$4.5997x10^{-6}$	$1.4547x10^{-6}$	$EuO_{1.13}F_{.73}$
30.00	4.418	1600	$4.0949x10^{-6}$	$1.2951x10^{-6}$	$EuO_{1.15}F_{.70}$
30.00	4.111	1603	$3.8128x10^{-6}$	$1.2106x10^{-6}$	$EuO_{1.17}F_{.67}$
30.05	3.909	1598	$3.6147x10^{-6}$	$1.1432x10^{-6}$	$EuO_{1.18}F_{.64}$
30.02	3.457	1597	$3.1989x10^{-6}$	$1.0117x10^{-6}$	$EuO_{1.19}F_{.61}$
30.00	3.336	1597	$3.0890x10^{-6}$	$9.7692x10^{-7}$	$EuO_{1.21}F_{.59}$
					$EuO_{1.22}F_{.56}$

III-D G.F. = 199.962 $a_o = 38.5x10^{-4}$

Time	μgEu	T°K	P_{EuF_2}	P_F	Composition
10.00	4.284	1651	$3.0833x10^{-5}$	$9.7513x10^{-6}$	$EuO_{1.10}F_{.78}$
10.05	3.713	1651	$2.6592x10^{-5}$	$8.4100x10^{-6}$	$EuO_{1.14}F_{.73}$
15.00	4.611	1652	$2.2132x10^{-5}$	$6.7148x10^{-6}$	$EuO_{1.16}F_{.67}$
25.00	6.333	1651	$1.8231x10^{-5}$	$5.7658x10^{-6}$	$EuO_{1.20}F_{.61}$
25.00	5.359	1655	$1.5446x10^{-5}$	$4.8850x10^{-6}$	$EuO_{1.25}F_{.51}$
30.00	4.111	1653	$9.8692x10^{-6}$	$3.1212x10^{-6}$	$EuO_{1.29}F_{.42}$

III-D (Continued)

Time	μgEu	T°K	P_{EuF_2}	P_F	Composition
40.00	4.984	1652	8.9708×10^{-6}	2.8371×10^{-6}	$EuO_{1.33}F_{.34}$
50.00	4.591	1654	6.6148×10^{-6}	2.0920×10^{-6}	$EuO_{1.38}F_{.24}$
60.00	4.452	1656	5.3486×10^{-6}	1.6915×10^{-6}	$EuO_{1.43}F_{.15}$
					$EuO_{1.48}F_{.05}$

Vap V-B G.F. = 203.12 $a_0 = 38.25\times10^{-4}$

pure EuOF

Time	μgEu	T°K	P_{EuF_2}	P_F
5.00	6.888	1783	1.0533×10^{-4}	3.3313×10^{-5}
5.00	5.350	1787	8.1916×10^{-5}	2.5907×10^{-5}
8.00	6.620	1785	6.3310×10^{-5}	2.0022×10^{-5}
10.00	5.584	1787	4.2749×10^{-5}	1.3520×10^{-5}
15.00	6.040	1785	3.0806×10^{-5}	9.7428×10^{-6}
15.01	4.917	1784	2.5054×10^{-5}	7.9238×10^{-6}
20.01	3.482	1784	1.3249×10^{-5}	4.1903×10^{-6}
20.00	1.071	1785	4.0959×10^{-6}	1.2955×10^{-6}

Vap V-A G.F. = 202.471 $a_0 = 38.25\times10^{-4}$

EuOF with excess b-Eu_2O_3

5.99	1.1863	1696	1.4722×10^{-5}	4.6561×10^{-6}
8.02	2.042	1719	1.9053×10^{-5}	6.0259×10^{-6}
8.00	2.369	1727	2.2211	7.0247
12.00	2.439	1726	2.1491	6.7965
12.00	3.020	1725	1.8866	5.9667

Vap V-A (Continued)

Time	μg	T°K	P_{EuF_2}	P_F
11.99	3.283	1724	2.0519	6.4892
15.00	3.876	1725	1.9372	6.1268
20.00	4.435	1724	1.6620	5.2564
20.00	5.003	1727	1.8765	5.9349

IV-B G.F. = 220.897 $a_o = 1.019\text{x}10^{-4}$

Time	μgEu	Temp	P_{EuF_2}	P_F	Composition
50.00	5.418	1524	$3.1278\text{x}10^{-6}$	$9.8919\text{x}10^{-7}$	$EuO_{1.00}F_{.99}$
50.02	4.651	1523	2.6328	8.4845	$EuO_{1.01}F_{.98}$
50.00	4.637	1522	2.6749	8.4595	$EuO_{1.02}F_{.97}$
50.00	3.638	1513	2.0929	6.6191	$EuO_{1.02}F_{.96}$
					$EuO_{1.03}F_{.95}$

IV-C G.F. = 221.343 $a_o = 1.019\text{x}10^{-4}$

25.00	4.635	1585	$5.4576\text{x}10^{-6}$	$1.7260\text{x}10^{-6}$	$EuO_{1.03}F_{.94}$
25.00	4.221	1580	4.9800	1.5750	$EuO_{1.04}F_{.93}$
25.00	3.762	1582	4.4236	1.3990	$EuO_{1.04}F_{.92}$
25.00	3.362	1583	3.9553	1.2509	$EuO_{1.05}F_{.91}$
					$EuO_{1.05}F_{.90}$

Appendix III

Thermodynamic Values

$EuF_{3(g)}$	Cp°	$H°_T-H°_{298}$ in cal	$S°_T$ in eu	fef eu
1500 K	14.811	17410	96.899	-85.293
1600	14.823	18892	87.856	-86.048
1700	14.832	20374	98.754	-86.930
1800	14.839	21858	96.611	-87.458

$EuF_{2(g)}$				
1500 K	13.841	16475	97.430	-86.543
1600	13.849	17715	98.323	-87.251
1700	13.856	19100	99.163	-87.928
1800	13.862	20486	99.954	-88.573

Free Energy Functions

Temp °K	$EuF_{3(s)}$	$EuOF_{(s)}$
1500	-50.809	-38.052
1600	-52.573	-39.068
1700	-54.337	-40.084
1800	-56.101	-41.100
1900	-57.865	-42.116

Appendix IV

Reactions of EuOF and EuF_3 with Cell Materials

Cell	Residue		Effusate	
	X-Ray Diffraction	X-Ray Fluorescence	X-Ray Diffraction	X-Ray Fluorescence
Mo + EuOF	White → Beige(EuOF + c-Eu_2O_3)	No Mo	Dark Brown - fcc a = 5.78 $\pm$ 0.01	Trace of
	Purple → Black (b-Eu_2O_3 bcc (a = 10.80 Å)	Mo	$EuF_{2.29}$-$EuF_{2.44}$	Mo
Mo + EuF_3	Orange fcc (a = 5.78) + EuF_3	Mo	Beige = $EuF_{2.29}$ → $EuF_{2.44}$ +? Phase	Mo
			Brown = ? Phase	Mo
Pt + EuOF (No M)	White - EuOF + c-Eu_2O_3	no Pt	Gold - $EuF_{2.50}$ + ? Phase	No Pt
Pt + EuOF in Mo cup	Pink - EuOF + c-Eu_2O_3	Mo	Brown (fcc, a = 5.78)	Trace Mo
		no Pt	$EuF_{2.29}$-$EuF_{2.44}$	No Pt
W + EuOF	Blue - b-Eu_2O_3 + bcc + bcc a = 10.76 Å	No Test	Not Collected	
ThO_2 + EuOF	Brown - a = 9.59, c = 7	No Th	Not Collected	
	Yellow - ? Phase	Th		

Appendix V

X-Ray Diffraction Analysis of Eu-Th Compound

$Eu_2Th_3(EuO_4)_3O$ a = 9.590 ± 0.002 c = 7065 ± 0.009

OBSERVED			CALCULATED		CALCULATED FOR $Eu_6(SiO_4)_3O$
$\sin^2\theta$	Relative Intensity	hkℓ	$\sin^2\theta$	Intensity	Intensity
		100	.0086	3.9	4.9
.02591	5	110	.0258	2.7	4.7
.03451	10	200	.0344	2.3	24.5
.03780	10	111	.0377	1.2	26.6
.04766	5	002	.0475	19.6	10.0
.05626	20	102	.0561	8.6	40.5
.06037	20	120	.0602	18.0	38.9
.07220	100	121	.0721	100.0	100.0
.07346	70	112	.0733	57.1	82.5
.07751	40	300	.0774	35.0	52.1
.8198	4	202	.0819	2.1	3.1
.10305	2	220	.1032	0.0	1.6
.11174	5	130	.1118	0.2	1.8
.12474	2	302	.1249	0.4	2.1
.13274	10	113	.1328	0.7	7.5
.13754	4	400	.1376	1.3	2.6
.15079	15	222	.1507	6.7	12.7
.15936	10	132	.1593	1.5	7.1

	OBSERVED			CALCULATED	CALCULATED FOR $Eu_6(SiO_4)_3O$
$\sin^2\theta$	Relative Intensity	hkℓ	$\sin^2\theta$	Intensity	Intensity
.16342	5	320	.1634	1.0	2.5
.16726	20	213	.1672	7.0	6.3
.17534	7	231	.1753	3.0	4.0
.18071	10	140	.1806	1.2	4.1
.18515	15	033	.1844	0.1	6.8
.19027	5	004	.1902	2.3	3.0
.22433	2	204	.2246	0.1	1.4
.22823	2	142	.2281	0.4	0.7
.24050	4	240	.2408	1.7	2.4
.24411	4	331	.2441	1.7	2.4
.25044	5	124	.2504	1.8	4.1
.26254	7	052	.2625	3.4	3.0
		150	.2666	1.0	1.5
.26713	8	304	.2676	3.8	4.9
.27033	8	323	.2704	2.5	3.8
.27888	5	151	.2785	3.2	4.1
		332	.2797	1.4	3.1
		404	.3278	0.6	1.2
.34719	2	251	.3473	1.4	2.1
		324	.3536	0.6	1.4
.35667	2	602	.3571	1.1	1.8
		125	.3574	2.9	2.4
		342	.3657	1.1	2.0
		160	.3698	0.9	1.0

OBSERVED			CALCULATED		CALCULATED FOR $Eu_6(SiO_4)_3O$
$\sin^2$	Relative Intensity	hk	$\sin^2$	Intensity	Intensity
.36968	2	414	.3708	1.3	4.4
		153	.3736	1.5	1.8
		161	.3817	0.2	1.4
.38208	7	252	.3829	0.9	3.8